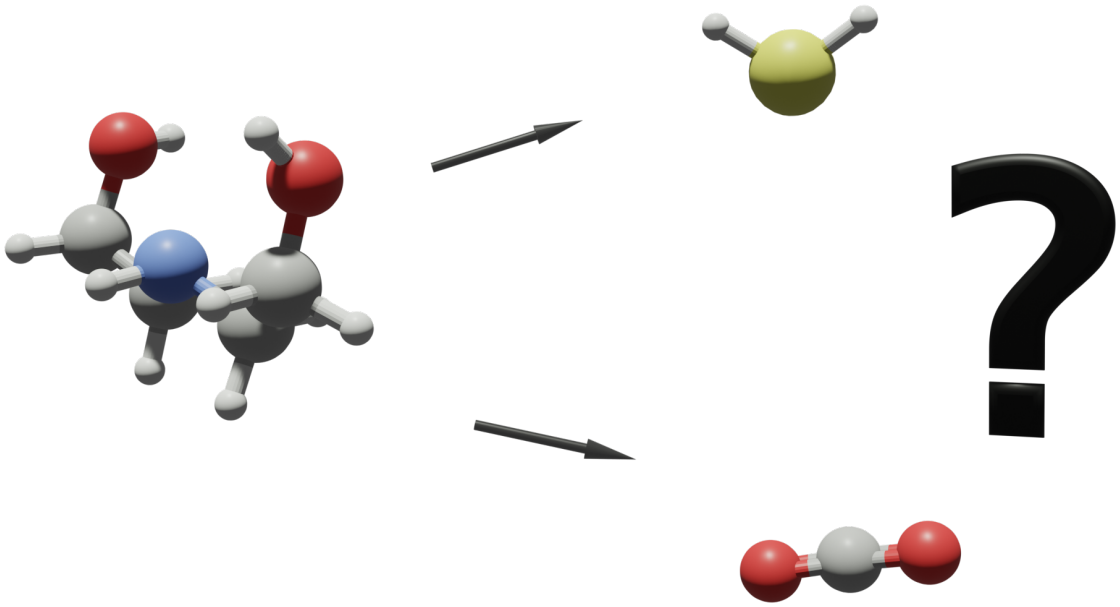

Selective and non-selective absorption of H_2S and CO_2 in amine treating units

Modelling and optimising amine units in an integrated refinery

Master's thesis in Sustainable Energy Systems

MELKER WIKSTRÖM

DEPARTMENT OF SPACE, EARTH AND ENVIRONMENT

CHALMERS UNIVERSITY OF TECHNOLOGY
Gothenburg, Sweden 2025
www.chalmers.se

DEGREE PROJECT REPORT 2025

Selective and non-selective absorption of H_2S and CO_2 in amine treating units

Modelling and optimising amine units in an integrated refinery

MELKER WIKSTRÖM

CHALMERS
UNIVERSITY OF TECHNOLOGY

Department of Space, Earth and Environment
CHALMERS UNIVERSITY OF TECHNOLOGY
Gothenburg, Sweden 2025

Selective and non-selective absorption
of H_2S and CO_2 in amine treating units
Modelling and optimising amine units in an integrated refinery
MELKER WIKSTRÖM

© MELKER WIKSTRÖM, 2025.

Supervisor: Karl-Martin Svan Hansson, St1 Refinery AB
Examiner: Gunnar Eriksson, Chalmers University of Technology

Degree project report 2025
Department of Space, Earth and Environment
Chalmers University of Technology
SE-412 96 Gothenburg
Sweden
Telephone +46 31 772 1000

Cover: Rendering of diethanolamine, hydrogen sulfide and carbon dioxide visualised in Blender. Molecules, atoms, or bonds are not true to size.

Typeset in LaTeX
Gothenburg, Sweden 2025

Selective and non-selective absorption of H_2S and CO_2 in amine treating units
Modelling and optimising amine units in an integrated refinery
MELKER WIKSTRÖM
Department of Space, Earth and Environment
Chalmers University of Technology

Abstract

This Master's thesis investigates the selective and non-selective absorption of hydrogen sulphide (H_2S) and carbon dioxide (CO_2) in amine treating units within a refinery setting. The study focuses on optimising the operation of these units to enhance the selective absorption of H_2S over CO_2 or the non-selective absorption of either, and thereby make the studied units more effective at their objectives. The thesis covers diethanolamine (DEA) and methyldiethanolamine (MDEA) and discusses the impact of various operating parameters, such as amine concentration and regenerator reboiler duty, on the absorption efficiency.

Experimental runs were conducted on two units: a Green Processing Unit (GPU) and a Tail Gas Treating Unit (TGTU). The results were compared with rate-based model predictions simulated with Aspen HYSYS. The findings indicate that it is not straightforward whether higher or lower amine concentration has an impact on the selectivity of DEA. However, reboiler duty in the GPU regenerator had no impact on absorber performance within the studied range, and no effect on selectivity; thus, operating at the lowest studied reboiler duty allows the refinery to save energy. For the TGTU which utilises MDEA, lowering the lean amine temperature was found to be effective in reducing CO_2 absorption while at the same time increasing the absorption of H_2S, thereby increasing selectivity.

Keywords: HYSYS, CCS, biofuels, sulphur recovery, industrial gas treatment, recycle gas scrubbing, process modelling, diethanolamine, methyldiethanolamine.

Acknowledgements

First and foremost, I would like to express my deepest gratitude to my supervisor, Karl-Martin Svan Hansson, for his unwavering support throughout this thesis. Your dedication and the countless hours spent explaining every detail have made this project immensely rewarding for me.

I extend a heartfelt thank you to the St1 laboratory, particularly the gas and water labs, for your significant contributions.

I am also grateful to Gunnar Eriksson for examining this thesis.

Lastly, I want to thank my partner, Sunna, for your support during the long hours spent on this project.

Melker Wikström, Gothenburg, May 2025

List of Acronyms

Below is the list of acronyms that have been used throughout this thesis, listed in alphabetical order:

DEA	dietanolamine
MDEA	methyl-dietanolamine
TGTU	Tail-gas treating unit
GPU	Green processing unit
HVO	Hydrogenated vegetable oil
FAME	Fatty acid methyl ester
SAF	Sustainable aviation fuel
VOC	Volatile organic compounds
CCS	Carbon capture and storage
SRU	Sulphur recovery unit
MEA	Monoethanolamine
DIPA	Di-2-propanolamine
AMP	2-amino-2-methyl-1-propanol
VLE	Vapour-liquid equilibrium
LPG	Liquid petroleum gasses
RGA	Refinery gas analyser
DCS	Digital control system
GC	Gas chromatography
HX	Heat exchanger

Contents

List of Acronyms ix

List of Figures xv

List of Tables xix

1 Introduction 1
- 1.1 Background . . . 1
- 1.2 Aim . . . 3
- 1.3 Limitations . . . 3
- 1.4 Specification of the issue being investigated . . . 3

2 Theory 5
- 2.1 Introduction to gas purification by amine treating . . . 5
- 2.2 Amines used in amine treating . . . 5
  - 2.2.1 Diethanolamine (DEA) . . . 5
  - 2.2.2 Methyldiethanolamine (MDEA) . . . 6
- 2.3 Absorption reactions in amine treating . . . 6
  - 2.3.1 Reactions with hydrogen sulphide . . . 7
  - 2.3.2 Reactions with carbon dioxide . . . 7
  - 2.3.3 Simultaneous absorption of carbon dioxide and hydrogen sulphide and amine selectivity . . . 8
- 2.4 Vapour-liquid equilibrium and enhancement factor . . . 8
- 2.5 Process modelling using HYSYS . . . 9
  - 2.5.1 Equilibrium modelling . . . 9
  - 2.5.2 Rate based modelling . . . 9
- 2.6 Process configuration of amine treating units . . . 11
- 2.7 Operation of amine treating units and important process parameters 13
  - 2.7.1 Amine feed rate . . . 13
  - 2.7.2 Absorber temperature approach . . . 13
  - 2.7.3 Amine concentration . . . 13
  - 2.7.4 Pressure in the amine regenerator and effect on amine degradation . . . 14
- 2.8 Operational constraints . . . 14
  - 2.8.1 Lean and rich amine pinched . . . 14
  - 2.8.2 Amine carry-over in absorber . . . 14

2.8.3 Amine carry-over in regenerator 15

3 Methods **17**
3.1 Sampling and method of analysis 17
3.1.1 Gas samples 17
3.1.2 Liquid samples 18
3.2 GPU test runs 19
3.3 TGTU test runs 20
3.4 Model setups 21
3.4.1 Fluid packages and reaction sets 21
3.4.2 Tower internals and solver settings 22
3.4.3 Considered components 22
3.4.4 GPU amine treating model 23
3.4.4.1 Absorber 24
3.4.4.2 Rich amine surge drum with flare gas absorber . . 24
3.4.4.3 Lean/rich heat exchanger 25
3.4.4.4 Amine regenerator 25
3.4.4.5 Lean amine air cooler 26
3.4.4.6 Makeup block and recycle 26
3.4.5 TGTU model 26
3.4.5.1 Absorber 27
3.4.5.2 Regenerator 29
3.5 Model parameter study 29

4 Results **31**
4.1 GPU experimental runs 31
4.1.1 Results 1: 31
4.1.2 Results 2: 32
4.1.3 Results 3: 33
4.1.4 Results 4: 34
4.1.5 Results 5: 35
4.2 Compiled GPU experimental and model results 36
4.2.1 Absorber and regenerator model results 36
4.2.2 Complete amine system model results 37
4.3 GPU operating parameter study 39
4.3.1 Amine concentration 39
4.3.2 Reboiler duty 41
4.4 Amine flow rate 42
4.5 TGTU test runs 43
4.5.1 Results 1: 44
4.5.2 Results 2: 44
4.6 Compiled TGTU experimental and model results 45
4.6.1 Sensitivity analysis of TGTU amine concentration 46
4.7 Results from model parameter study 48

5 Discussion **51**
5.1 Can selectivity be improved by changing operating conditions? . . 51

5.2 How much can the results from experimental runs and modelling of the GPU plant transfer to the TGTU absorber and potentially increase its selectivity towards hydrogen sulfide? 51
5.3 Impact of regenerator reboiler duty on absorber performance . . . 52
5.4 Which combination of operating parameters should be run on the amine units? 52
5.5 Liquid carry-over in amine regenerators 53
5.6 Problems with analysis method for ammonium in reflux water . . . 53
5.7 Sensitivity analysis of gas flow meters and excessive flashing in rich amine drum 54
5.8 Modelling the regenerator by steam to the reboiler flow rate or the reflux flow rate 55
5.9 Can the same model predict different operating scenarios? 57

6 Conclusions **59**

7 References **61**

A Calculations **I**
A.1 Nomenclature I
A.2 DEA loading (mol(gas)/mol(amine)) from concentration I
A.2.1 Amine mole count I
A.2.2 Rich and lean amine sour gas loading II
A.2.3 Assumptions III
A.3 Corrected flows from DCS III

B Detailed process diagrams **V**

C Column and model internals **IX**

D Model parameter study **XI**

E Elemental sulphur estimation from tank levels **XV**

List of Figures

2.1 Molecular structure of diethanolamine (DEA). 6
2.2 Molecular structure of methyldiethanolamine (MDEA). 6
2.3 Typical amine treating unit configuration where flows are labelled with names. 11
2.4 St1 GPU amine treating unit process diagram. The amine unit is of a third party design. A larger version can be found in Appendix B. 12
2.5 St1 tail gas treating unit process diagram. A larger version can be found in Appendix B. 12

3.1 GPU model flowsheet in HYSYS, where the main parts of the model can be seen. 24
3.2 GPU rich amine surge drum with flare gas absorber sub-model in HYSYS. 25
3.3 TGTU model setup in HYSYS, where the main parts of the model can be seen. 27
3.4 Process flow diagram of the different streams used for the mass balance around the TGTU. 27

4.1 Absorber efficiency, plant and model results plotted over the test runs. 37
4.2 Regenerator efficiency, plant and model results plotted over the test runs. 37
4.3 Absorber efficiency for the complete system, plant and model results plotted over the test runs. 38
4.4 Complete system: Regenerator efficiency, Plant vs model. 38
4.5 CO_2 removal and H_2S slip for the absorber plotted against amine concentration. Dotted lines are regression trends for GPU GC analysis and GPU H2S analysis. Mixed lines are regression lines for model predictions. 39
4.6 CO_2 removal and lean DEA H_2S loading for the regenerator plotted against amine concentration. Dotted lines are regression trends for experimental results. Mixed lines are regression lines for model predictions. 40
4.7 Sensitivity study on Test run 4 where amine concentration is changed. 40

4.8 CO_2 removal and H_2S slip for the absorber plotted against ratio between steam flow rate and lean amine flow rate. Dotted lines are regression trends for GPU GC analysis and GPU H2S analysis. Mixed lines are regression lines for model predictions. 41
4.9 CO_2 removal and lean DEA H_2S loading for the regenerator plotted against ratio between steam flow rate and lean amine flow rate. Dotted lines are regression trends for experimental results. Mixed lines are regression lines for model predictions. 42
4.10 Simulated amine flow rate changes based on GPU test run 5 plotted against absorber CO_2 removal and H_2S slip at fixed reboiler duty. 43
4.11 Simulated amine flow rate changes based on GPU test run 5 plotted against regenerator CO_2 removal and lean amine H_2S loading at fixed reboiler duty. 43
4.12 Absorber efficiency, TGTU vs model. 46
4.13 Regenerator efficiency, TGTU vs model. 46
4.14 Sensitivity analysis on amine concentration for TGTU. 47
4.15 Viscosity of the rich amine plotted against he acid gas loading of the rich amine. Viscosity decreases when the acid gas loading decreases. 47
4.16 Results from the model parameter study where CO_2 removal over the absorber is plotted against the test runs. 48
4.17 Results from the model parameter study where H_2S slip after the absorber is plotted against the test runs. 48
4.18 Results from the model parameter study where CO_2 removal over the regenerator is plotted against the test runs. 49
4.19 Results from the model parameter study where lean DEA H_2S loading after the regenerator is plotted against the test runs. Note that the unit is in mol/mol. 49

5.1 Amine concentration in reflux water plotted against reported ammonium concentration. 54
5.2 Calculated flows from mass balance compared to corrected measured flows from the DCS. Note that the mass balance flow for test run 5 is based on the Dräger analysis, since the GC analysis was unpredictable. 1 is perfect, where the mass balance and corrected gas flows are equal. 55
5.3 Plot where on the left-hand side the regenerator solo models for the GPU test runs are specified by the steam flow rate, and the resulting reflux flow ratio is plotted on the same axis. On the right-hand side, the same procedure is done after trusting the reflux flow rate. 56
5.4 Plot where the regenerator performance for both CO_2 and H_2S is plotted after either trusting the steam flow meter or the reflux flow meter. The model results can then be compared against the experimental results. 57

B.1 St1 GPU amine treating unit process diagram. The amine unit is of a third-party design. VI
B.2 St1 tail gas treating unit process diagram. VII

E.1 Process data of pit emptying. XV

List of Tables

1.1 Results from a performance test on the original TGTU unit at St1 Refinery. 2

3.1 Gas samples with names and process description. 17
3.2 Liquid samples with names and sampling position. 18
3.3 List of analysis and standards used. 18
3.4 Overview of the GPU test runs. 19
3.5 Overview of the TGTU test runs. 21
3.6 Components used in the GPU amine unit simulation. 23
3.7 Components used in the TGTU simulation. 23
3.8 Calculated values from TGTU mass balance. 29

4.1 Results from GPU run 1: 31
4.2 Results from reflux sample in GPU run 1: 32
4.3 Results from GPU run 2: 32
4.4 Results from reflux sample in GPU run 2: 33
4.5 Results from GPU run 3: 33
4.6 Results from reflux sample in GPU run 3: 34
4.7 Results from GPU run 4: 34
4.8 Results from reflux sample in GPU run 4: 35
4.9 Results from GPU run 5: 35
4.10 Results from reflux sample in GPU run 5: 36
4.11 Results from TGTU run 1: 44
4.12 Results from reflux sample in TGTU run 1: 44
4.13 Results from TGTU run 2: 45
4.14 Results from reflux sample in TGTU run 2: 45

5.1 Direct comparison between steam to reboiler/lean amine flow ratio and absorber performance between comparable runs. 52

C.1 Specification of models and unit internals. IX

D.1 Raw data from model parameter study. XI

1

Introduction

The process of removing hydrogen sulphide (H_2S) from gas streams with aqueous amine solutions is a well-established technology, used for many applications. For fossil refinery operators, tail-gas-treating units (TGTUs) have in the latter decades become a common addition to many refineries, which have contributed to increasing the sulphur recovery from around 90% to over 99%. [1, 2]. More recently, amines have had renewed interest since they play a vital role in absorbing carbon dioxide (CO_2) from flue gases in post-combustion CCS technology, which is seen as a potential way for refinery operators to mitigate emissions [3]. However, the fuel market is changing, and less carbon-intensive fuels are in increasing demand.

Fuels derived from bio-based feedstocks serve as an alternative to fossil fuels. These feedstocks differ in their composition compared to traditional crude oil, as they contain more oxygen. Hydrogenated vegetable oil (HVO) is a biodiesel that has similar properties to fossil diesel, which increases the compatibility with the current vehicle fleet [4, 5]. A not-so-insignificant bonus of HVO production is that it can be adapted to produce sustainable aviation fuel (SAF), which can aid in greatly reducing the CO_2 emissions from the aviation industry [6, 7].

1.1 Background

At St1 Refinery, there is a new green processing unit (GPU) started up in January 2024. The unit is very flexible and uses different fatty residues to produce either HVO or SAF. The feedstock can be both corrosive crude fatty acid (CFA) from the forest industry or used cooking oil (UCO), based on plant-based oils or animal fat. The unit is a modified catalytic hydrotreater process, derived from a fossil counterpart [6]. CO_2 and H_2S are both found in the process recycle gas, and these gases need to be continuously removed by a circulating diethanolamine (DEA) solution, for the unit to operate properly. St1 has seen the potential of reducing the reboiler duty of the GPU amine unit regenerator, which is used to strip sour gases from the circulating DEA solution. This can help reduce cost and energy usage.

The refinery has another unit, a TGTU, where there is a similar mixture of CO_2 and H_2S in the gas. Here, a selective absorption is requested such that H_2S is picked up, but as much as possible of the CO_2 slips through. This unit utilises an-

other amine, methyldiethanolamine (MDEA), that is more selective towards H_2S [8]. On the TGTU unit, there is currently a problem where high absorption rates of CO_2 cause accumulation of CO_2 in the sulphur recovery unit (SRU). This may be linked to problems with higher-than-normal H_2S slip from the tail gas absorber.

The TGTU amine absorber was originally designed to use DEA solution from the existing amine loop at the refinery. The amine bed was made short to avoid too much CO_2 pick-up. In the original unit, CO_2 was produced in the SRU in its fuel-fired line burners. Results from a performance test, seen in Table 1.1, indicated that about three-quarters of the CO_2 going into the absorber was absorbed and returned to the inlet of the SRU.

Table 1.1: Results from a performance test on the original TGTU unit at St1 Refinery.

Test	**A**	**B**
Sour Gas rate dry basis (kmol/h)	32,3	31,7
Sour gas temp (°C)	32,6	31,8
Sour gas H2S (mol%, dry basis)	1,328	1,173
Sour gas CO2 (mol% dry basis)	23,94	24,57
Sweet gas temp (°C)	50,0	49,0
Sweet gas H2S (ppm mol, dry basis)	298	174
Sweet gas CO2 (mol%, dry basis)	7,686	7,063
Lean amine rate (T/D)	205	205
Lean amine temp (°C)	48,0	47,5
H2S pick-up (%)	98,2	98,8
CO2 pick-up (%)	74,0	77,0

The original TGTU absorber were designed with a 3150 mm long Sulzer Mellapak M250Y structured packing ran at atmospheric pressure, paired with a common amine regenerator with nominal 30 wt% DEA.

After St1 bought the refinery, it was decided to revamp the TGTU. The line burners were replaced by electrical heaters, the amine absorber was given a higher packed bed with a packing material that could handle higher amine flows (4578 mm of Sulzer MellapakPlus M202.Y). A new amine regenerator was built for the TGTU, which meant that the amine used in the TGTU could be switched to a more selective one, MDEA at nominal 30 wt%. An online analyser for H_2S in the sweet gas from the TGTU absorber was installed. After start-up, H2S concentration in the sweet gas dropped to $\sim$1 ppm. When the GPU was built, acid gas from the GPU amine regenerator was routed to the gas inlet of the TGTU amine absorber, to absorb H_2S and slip CO_2.

1.2 Aim

The aim of this thesis is to study how the units should be operated to excel at their objectives. For the GPU unit, the target is finding an optimal combination of amine concentration and regenerator reboiler duty which meets the expected 99% absorption of H_2S and around 90% CO_2 from the recycle gas loop. Currently, the unit is run using trial and error and St1 is not sure whether the optimum operating conditions are found.

For the TGTU unit, the aim is to maximize the H_2S absorption and minimize the CO_2 absorption. Operating cost of the unit is of secondary interest here, since the unit's purpose is to reduce emissions to the atmosphere.

1.3 Limitations

The following list explains which issues are not addressed in this work, or what parts that may be removed from the scope.

1. The literature study on equilibrium and kinetics of amines will not cover other amines than DEA and MDEA since these are the amines that are currently in use at St1 Refinery.

2. St1 Refinery operates a third amine unit where multiple absorbers share the same regenerator. This unit will only be covered if a particular interest in a specific issue arises, since it has a lot more complexity.

1.4 Specification of the issue being investigated

Questions to be answered during the thesis are:

1. How much can changing operating parameters affect DEA's selectivity towards H_2S or CO_2?

2. Which combination of operating parameters for the GPU unit amine loop provides sufficient absorption, while minimising energy use?

3. How much can the results from experimental runs and modelling of the GPU plant transfer to the TGTU absorber and potentially increase its selectivity towards H_2S?

4. What parameters can further increase the selectivity in the TGTU unit towards H_2S?

5. How close can a computer model predict the DEA loadings and gas compositions for more than one operating condition for the GPU absorber and regenerator?

In this section, operating parameters consider lean amine flow, lean amine temperature, amine concentration and regenerator reboiler duty for the GPU amine loop. Amine concentration and regenerator reboiler duty will be tested by experiments, and other parameters will be tested by model parameter studies.

2

Theory

This chapter will cover the theory of amine gas treating, including principles of absorption, chemical reactions, types of amines, factors influencing absorption rate, and process design considerations, including short descriptions of the considered amine units covered in the thesis.

2.1 Introduction to gas purification by amine treating

Gas purification is the process of removing vapour-phase impurities from gaseous streams. Impurities can include hydrogen sulphide (H_2S), carbon dioxide (CO_2), water vapour, sulphur dioxide, nitrogen oxides and volatile organic compounds (VOCs) [9]. There are various processes used commercially to do this, ranging from simple water washes to advanced multi-stage adsorbers.

A widely used technology is amine treating, which utilises aqueous solutions of alkanolamines like monoethanolamine (MEA), diethanolamine (DEA), di-2-propanolamine (DIPA), and methyldiethanolamine (MDEA) to absorb impurities from gas streams. Common applications are in natural gas sweetening units where the amine washes out CO_2 and H_2S to meet stringent product specifications and reduce corrosion in transport. It is also used by refiners to selectively wash out impurities from hydrotreating units that otherwise would accumulate in processes and in tail gas treating units (TGTUs) to reduce sulphur emissions by treating sulphur recovery unit (SRU) tail gases.

2.2 Amines used in amine treating

In this section, amines that are considered in this thesis will be explained further.

2.2.1 Diethanolamine (DEA)

Diethanolamine (DEA) is a secondary amine that has been used to sweeten sour gas streams successfully for almost a century. The first successful large-scale pilot plant was constructed in the 1930s [10]. Aqueous solutions of DEA are often

used to remove CO_2, H_2S and other acidic gases from gas streams, which are absorbed to the amine group seen in Figure 2.1:

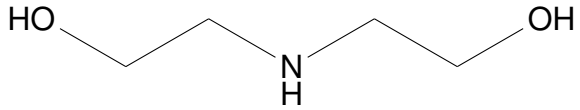

Figure 2.1: Molecular structure of diethanolamine (DEA).

Special characteristics that DEA have, compared to primary amines like MEA, is that DEA is less reactive to common SRU contaminants such as COS and CS_2 and have a much lower vapour pressure, which minimises vaporisation, allowing for low-pressure operations. DEA requires low pressure in the regenerator, since it degrades at higher temperatures. These degradation products can be corrosive [9].

2.2.2 Methyldiethanolamine (MDEA)

Methyldiethanolamine (MDEA) is a tertiary amine that has successfully been used to selectively treat sour gas streams since the 1950s [11]. It owes its selectivity towards H_2S, because it has a methyl group that acts as a steric hindrance, seen in Figure 2.2:

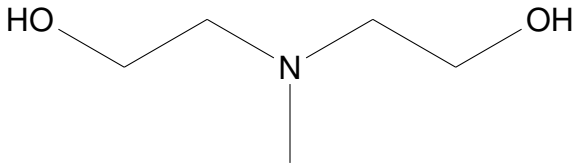

Figure 2.2: Molecular structure of methyldiethanolamine (MDEA).

The higher steric hindrance compared to DEA makes MDEA react very slowly with CO_2 but as fast or faster with H_2S. Another advantage is that MDEA have lower regeneration energy than DEA [12]. mDEA is reported to have better resistance to chemical degradation compared to DEA and MEA [9].

2.3 Absorption reactions in amine treating

Chemical absorption is the combined phenomenon of gas mass transfer into a bulk liquid phase and the chemical reaction that occurs inside the bulk phase [13]. The mass transfer is often described through a two-film theory, where the sour gas is transferred from the gas phase onto an interface and then further into the bulk of the amine solution. The chemical reactions are most often described by a rate model [14]. From now on, absorption mentioned in this thesis will always be chemical absorption.

The reaction mechanisms will differ depending on which gas the amine is reacting with and what chemical structure the amine has. Typically, amines are divided into primary, secondary and tertiary structures, depending on how many substituents are bonded to the amine group. A common primary amine is monoethanolamine (MEA), a common secondary amine is diethanolamine (DEA) and a common tertiary amine is methyldiethanolamine (MDEA). Another important property is whether the amine is sterically hindered, which essentially means how hard it is for a reactant to reach the amine group on the molecule.

2.3.1 Reactions with hydrogen sulphide

Secondary amines react with H_2S as seen in Equation 2.1a and tertiary amines react with H_2S as seen in 2.1b. Both reactions are an almost immediate proton transfer [15].

$$H_2S + R_2N \leftrightarrow HS^- + R_2NH_2^+ \tag{2.1a}$$

$$H_2S + R_3N \leftrightarrow HS^- + R_3N^+H \tag{2.1b}$$

In practice, this means that the rate of H_2S absorption in amine treating most often is limited by equilibrium or sometimes mass transfer.

2.3.2 Reactions with carbon dioxide

Primary and secondary amines are believed to have the same reaction with CO_2 at low concentrations, where they form a zwitterion upon contact (Equation 2.2a) which then forms a carbamate complex (Equation 2.2b) and then further react with a water molecule (Equation 2.2c) [16, 17, 18].

$$RR'NH + CO_2 \leftrightarrow RR'NH^+COO^- \tag{2.2a}$$

$$RR'NH^+COO^- + RR'NH \leftrightarrow RR'NCOO^- + RR'NH_2^+ \tag{2.2b}$$

$$RR'NCOO^- + H_2O \leftrightarrow RR'NH + HCO_3^- \tag{2.2c}$$

Tertiary amines, such as MDEA, are believed to not react directly with CO_2 due to the lack of a free hydrogen atom, but instead forms a bicarbonate catalysed by a base instead, see Equation 2.3 [17, 19].

$$R_3N + H_2O + CO_2 \leftrightarrow R_3N^+H + HCO_3^- \tag{2.3}$$

However, the observed kinetics between researchers varies a lot [17, 18, 19, 20]. Donaldson [17] was the first to believe that both primary and secondary amines react in a more complex manner [19]. Said et al. [21] propose that the old four-membered mechanism described in Equation 2.2 and 2.3 has too high of an energy barrier, and propose a new unified six-membered mechanism. Essentially, the new mechanism proposes that a Lewis base does a nucleophilic

attack on the CO_2, assisted by a Brønsted base. The assist is done by facilitating a proton transfer/exchange. Other amines, water, or hydroxyl groups can act as the Brønsted base or the Lewis base and depending on the conditions and different reaction products are generated. This new mechanism suggests that many parameters can affect how efficient the CO_2 absorption is.

2.3.3 Simultaneous absorption of carbon dioxide and hydrogen sulphide and amine selectivity

Simultaneous absorption is harder to understand, since essentially two gasses compete for the same active proton on the amine. For sour gas treating, the reactions with CO_2 and H_2S have wildly different characteristics, which adds complexity, but also possibilities for a selective absorption.

Since reaction between H_2S and amines are almost instant and the reaction with CO_2 is multitudes slower, longer contact times always yields a higher CO_2 loading.

As H_2S absorption is mass transfer limited and CO_2 is reaction rate limited, reactivity with H_2S decreases with higher temperature, and reactivity increases with CO_2 [15]. This would indicate that at a higher temperature, the CO_2 absorption is faster and therefore more eager to compete for the reaction proton.

Some claim that higher concentrations of amines have indicated a decrease in selectivity towards H_2S and therefore increase CO_2 absorption. This could be due to CO_2 absorption being kinetically limited, and at higher concentrations of amine in the bulk phase would generate more reactions [22, 23]. Effects of amine concentration are further discussed in Subsection 2.7.3.

In secondary amines, such as MDEA, the liquid phase can initially be saturated with H_2S due to the rapid uptake at the beginning of the absorption process. This quickly changes the pH of the solution, from slightly basic to more acidic, and decreases the available protons. This can lead to a higher equilibrium vapour pressure of H_2S than the partial pressure of H_2S in the bulk gas phase, which reverses the driving force and lets the absorbed H_2S desorb back onto the gas phase [24]. This phenomenon has been observed in industrial operations and indicates that a longer residence time in the absorber would decrease selectivity towards H_2S [25, 11].

2.4 Vapour-liquid equilibrium and enhancement factor

Vapour-liquid equilibrium (VLE) is the relationship between the concentration of acid gases in an amine solution and its partial pressure in the gas phase [9]. Note that the VLE considers all solved gases, not just the gases loaded onto the amine, since the water contributes as well.

Film theory is a model used to describe mass transfer phenomena in gas-liquid systems. It states that the resistance to mass transfer exists in thin films on either side of the gas-liquid interface. It assumes that equilibrium exists at the interface, as defined by Vapour-Liquid Equilibrium (VLE) and often described by Henry's Law. The driving force for mass transfer is the concentration difference across these films [9].

In amine treating, the absorption of acid gases (CO_2, H_2S) into amine solutions is often accelerated by chemical reactions. The enhancement factor is used to quantify the increase in the mass transfer rate due to these reactions. It adjusts the overall mass transfer coefficient to account for the impact of the reaction [9, 26].

Another important aspect is the equilibrium solubility, to what extent an amine will absorb in equilibrium with a certain sour gas. This differs between sour gases, but importantly it differs when the gases are present together, since both gases are fighting over the same proton [27].

Understanding the concepts of VLE and enhancement factors is fundamental for accurate simulation of amine treating processes. These principles are embedded in the models used by simulation tools like Aspen HYSYS, where thermodynamic equilibrium and mass transfer rates are incorporated either through simplified assumptions (equilibrium models) or through detailed kinetic and transport models (rate-based approaches).

2.5 Process modelling using HYSYS

HYSYS Acid Gas Cleaning package utilises a technology which is based on the electrolyte NRTL model for electrolyte thermodynamics and Peng-Robinson Equation of State for vapour phase properties [28].

HYSYS utilises equilibrium and rate data from multiple sources, but does not use data for MDEA reported by Jou et al. since their results do not agree with the other papers on kinetics [29, 30, 31, 32]. A full list of used equilibrium data in HYSYS is provided in AspenTech's white paper *Acid Gas Cleaning Using Amine Solvents: Validation with Experimental and Plant Data* [28].

2.5.1 Equilibrium modelling

Equilibrium modelling utilises stage efficiencies, which means the user needs to specify a stage efficiency which states how far the equilibrium will pass at each stage [33]. This is an empirical approach.

2.5.2 Rate based modelling

Rate-based modelling utilises heat and mass transfer correlations based on its transfer properties and tray or packing geometry, where multiple components are

considered, their interactions and their chemical reactions [33]. The chemical reactions are especially important when modelling amine treating units, since the reactions enhance the mass transfer between the liquid and vapour phase [34].

Aspen HYSYS utilises two different rate-based technologies, one of which utilises a classic equilibrium-stage model to solve the column, but calculates a rate-based efficiency for CO_2 and H_2S at each stage. The other technology, called the *Advanced method*, utilises the Maxwell-Stefan theory of mass transfer in regions defined by film theory, to calculate heat and mass transfer rates without assuming either chemical or thermal equilibrium between vapour and liquid. The latter technology is better suited if the process gas is contaminated with other gases than CO_2 and H_2S [28].

2.6 Process configuration of amine treating units

In a typical amine treating unit, there is an absorber (sometimes called a scrubber), a regenerator (sometimes called a stripper), one or many heat exchangers and a reboiler. Aqueous solution of lean amine is pumped into the absorber from the top, while the sour gas stream that is to be treated enters from the bottom. The amine then absorbs sour gases from the inlet gas stream while flowing downwards in the absorber to then exit from the bottom. This amine is now rich in carried sour gases and sent to the regenerator. In the regenerator, the rich amine is heated with a reboiler, stripping off the sour gases. The sour gases are typically fed to a sulphur recovery unit (SRU), or in the case of a TGTU it is sent to an incinerator and further released to the atmosphere. The now lean amine is pumped back to the absorber. Typically, there is a heat exchanger which heats the rich amine and cools the lean amine before entering the units and some sort of cooler which cools away the accumulation of heat in the system. A simple process diagram can be seen in Figure 2.3.

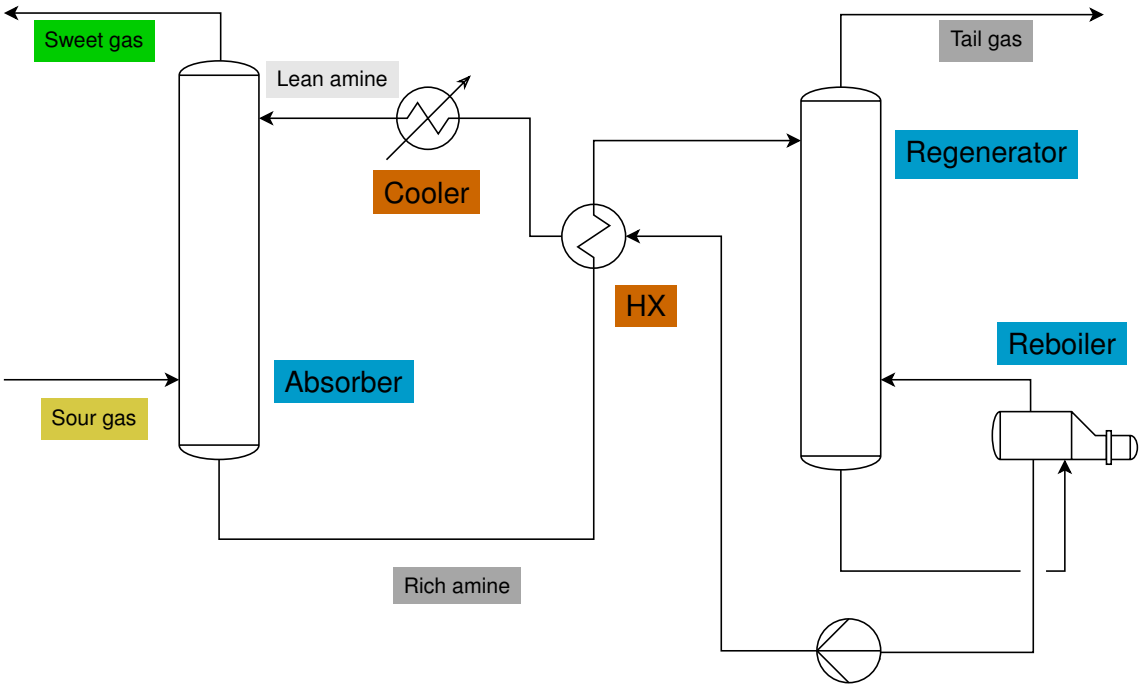

Figure 2.3: Typical amine treating unit configuration where flows are labelled with names.

The considered GPU amine treating unit at St1 Refinery in Gothenburg has a different configuration, seen in Figure 2.4. The process adds surge drums for both lean and rich amine. The rich amine drum doubles as a flash drum, where hydrogen and light hydrocarbons, which are dissolved in the solution can flash off. Some liquid can be entrained with these gases. These flash gases are cleaned through a very small absorber, which is continuously washed with lean amine. Low-density hydrocarbons that float on top of the aqueous phase can be pumped out through a hydrocarbon separating pocket. In addition to the flare gas absorber

and the main recirculation gas absorber, the amine unit serves a third small absorber which is used to clean LPG from the GPU unit, which is marked in the figure as “DEA to other consumers”. This is a very small part of the amine feed rate.

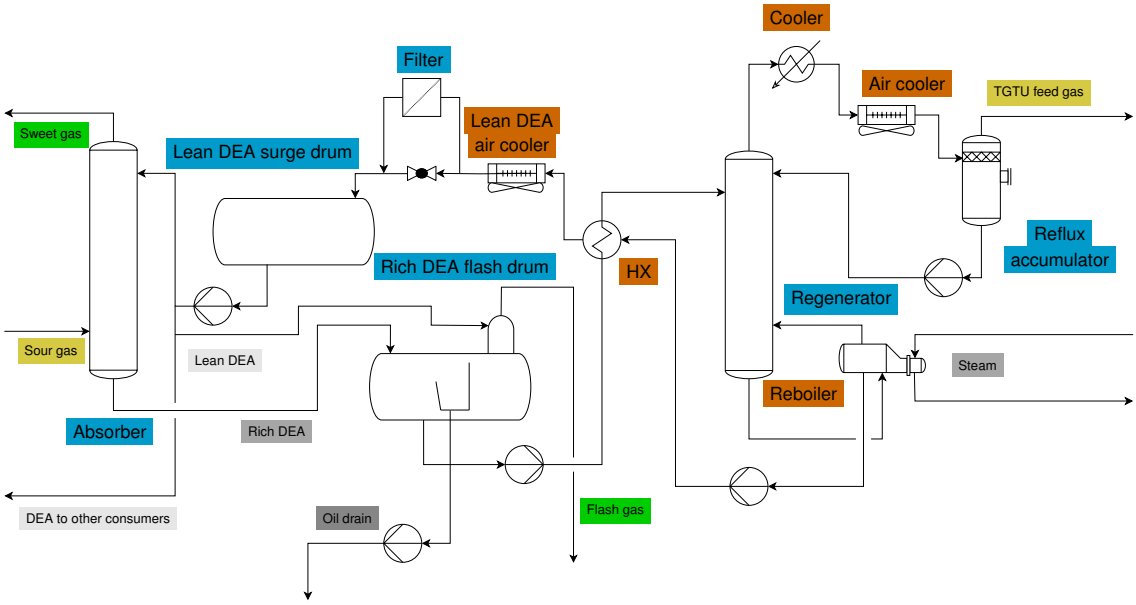

Figure 2.4: St1 GPU amine treating unit process diagram. The amine unit is of a third party design. A larger version can be found in Appendix B.

The St1 TGTU is more similar to the typical amine treating unit from Figure 2.3 with a lean amine surge drum. The process can be seen in Figure 2.5:

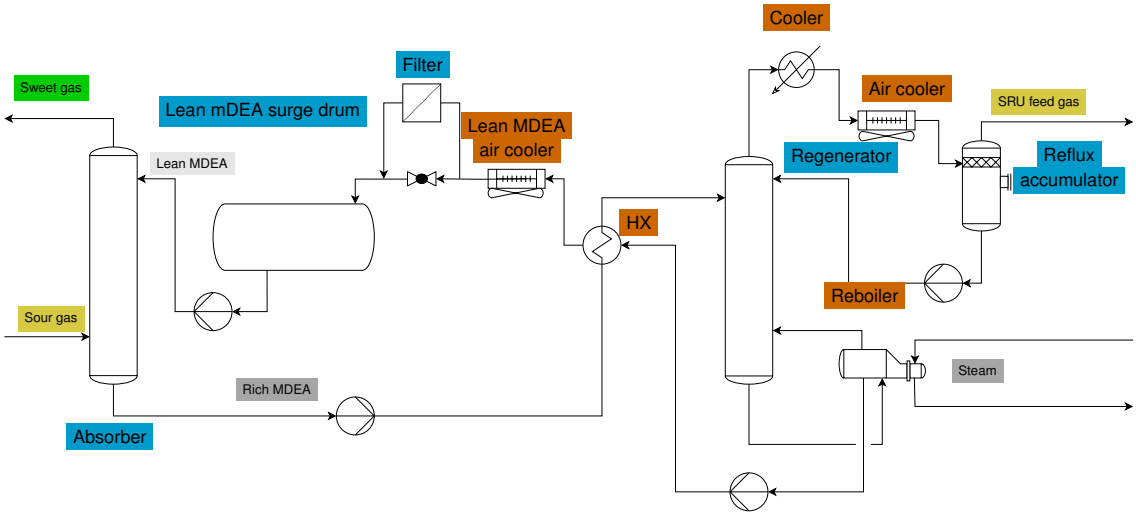

Figure 2.5: St1 tail gas treating unit process diagram. A larger version can be found in Appendix B.

Both units have a filter setup, which has both particulate filters and activated carbon filters. These continuously filter out impurities and degradation byproducts.

2.7 Operation of amine treating units and important process parameters

In this Section, key operational parameters and their impact on the process are further discussed. This does highlight a couple of challenges and methods to reduce costs and energy usage.

2.7.1 Amine feed rate

Amine feed rate is the circulation rate of the aqueous amine solution leaving the regenerator and entering the absorber. Increasing the amine feed rate to the absorber potentially increases the absorption, if the process is rich amine pinched (see Subsection 2.8.1). This will however, increase the reboiler duty, since more amine needs to be heated by the regenerator reboiler. The amine feed rate can be limited by hydraulic limits in the process equipment. Increasing the amine feed rate can be compared to increasing the amine concentration, both increase the amine mole count entering the absorber. However, changing the concentration does change the chemical and physical properties of the aqueous mixture, but either way, the amine feed rate should be optimised together with the amine concentration to get the best absorption in the absorber and the least reboiler duty.

2.7.2 Absorber temperature approach

Temperature difference between the lean DEA to the inlet of the absorber to the inlet sour gas feed heavily affects absorption. Lower temperatures increase equilibrium solubility especially for H_2S in the aqueous amine solution. If the temperatures get dramatically higher, increased amine degradation is a potential problem. Higher temperatures negatively affect selectivity between H_2S and CO_2 further explained in Subsection 2.3.3. Lean amine temperature is regulated using a cooler before the absorber amine inlet.

2.7.3 Amine concentration

Higher concentrations usually yield higher sour gas absorption due to more active amine that can react with sour gases, but if the concentrations are too high, the amine can be too viscous, which results in poor diffusion of gases. CO_2 absorption is negatively affected by this [35]. Higher amine concentrations do affect selectivity since the competition for lean amine is limited, which usually leads to increased absorption of the slower reacting gas, in most cases CO_2 [15, 23, 36]. If one would design an amine treating unit with a very low H_2S slip (less than 5 ppm) a high amine concentration may be needed, however, this would result in a lower selectivity towards H_2S and more CO_2 absorption, therefore much care and consideration should be put into determining the amine concentration for a unit.

2.7.4 Pressure in the amine regenerator and effect on amine degradation

Higher pressure in the amine regenerator requires a higher temperature for the reboiler to successfully dissociate the bond between the sour gases and the amine. The following higher temperature does increase amine degradation as well, which produces unwanted byproducts and requires expensive amine make-up [9]. At 135°C in the absence of CO_2, only 3% degradation was observed after 4 weeks by Saeed et al. [37]. If CO_2 is present, DEA degradation starts at 100°C, and is accelerated with higher temperatures; however, to what extent is not very certain [38, 37].

2.8 Operational constraints

In this section, known operational constraints of amine treating units which are relevant to this thesis will be presented.

2.8.1 Lean and rich amine pinched

Normally when operating amine treating units there are two constraints that can occur where either the lean amine is pinched or the rich amine is pinched.

Lean amine pinched occurs when the lean amine is in equilibrium with the sweetened gas. The only way to solve this is by increasing the driving force, which can be done in multiple ways, for example, by having a leaner amine or decreasing the temperature. The opposite is rich amine pinched, which occurs when the amine reaches equilibrium too fast in the absorber, resulting in the amine being saturated fully before all gases are absorbed. This could happen when the lean amine flow onto the absorber is too small or when the amine concentration is too low.

To make it easier to understand, lean amine pinched is like washing clothes that already have been washed, they will not get cleaner, if you run the machine on the same settings again. Rich amine pinched is like you add too little water or too little detergent and the clothes come out of the washing machine dirty and if you try to run the washing machine again with the same water it will not get cleaner.

2.8.2 Amine carry-over in absorber

A potentially too high flow of gas or sometimes amine to the absorber can result in severe carry-over of amine to the recirculation gas knock-out drum, potentially stopping the recirculation gas compressor. This carry-over is potentially due to excessive hydraulic loading of the absorber or by contaminants in the process gas [39].

2.8.3 Amine carry-over in regenerator

Some previous case studies mention problems with amine carry-over, which means that the aqueous phase entering the amine regenerator is entrained into the gaseous phase and subsequently carried into the condenser, resulting in around 20% amine in the reflux water (Lieberman does not mention if it is by volume or by weight). In Lieberman's case study, the amine was probably entrained due to severe corrosion, which led to a high pressure drop resulting in flooding [40]. In Nag's case study, the reason was probably poor performance in the upper wash trays due to low liquid loads, which resulted in liquid level loss. This allowed vapour to bypass the trays altogether, entraining the amine solution. This resulted in similar amine concentration in the reflux water as in the amine circulated. The issue was resolved by installing gaskets with seal welds in the wash section. Nag does discuss if foaming could have been a contributing factor as a result of an increased pressure drop across the column [41].

3

Methods

This chapter outlines the methodology used in the thesis. It begins with a description of the sampling procedures and the methods of analysis. This is followed by a presentation of the test runs and the corresponding process parameters at the time of sampling. Next, the setup and specification of the model are detailed. Finally, a parameter study is presented, comparing different mass transfer and tray models.

3.1 Sampling and method of analysis

In this section, details of the sampling and analysis methods will be presented.

3.1.1 Gas samples

Gas samples were gathered in closed sample cylinders, which were thoroughly flushed before filling. The samples were filled at a slightly throttled pressure compared to the process pressure to avoid partial condensation inside the cylinder. This method was used for the following samples according to Table 3.1.

Table 3.1: Gas samples with names and process description.

Name in thesis	Process description
GPU sour gas	Recirculation gas before absorber
GPU sweet gas	Recirculation gas after absorber

The composition of the gas samples were analysed with a refinery gas analyser (RGA) according to standard SS-EN 15984, which is a chromatographic method. The samples were either run on RGA analyser 1 or RGA analyser 2. What analyser have been used can be seen in tables with gas results.

Since hydrogen sulphide was lower than the detection ranges of the RGA apparatus, Dräger tube analysis was carried out on all samples. On most samples, Dräger tube analysis was done for carbon dioxide concentration as well, to verify the RGA analysis.

3.1.2 Liquid samples

Both lean and rich DEA and MDEA were sampled in glass bottles using cork caps, which were filled up into the neck to avoid excessive flashing of gases in the bottles. The sampling system, which was of Dopak style, was flushed through two bottles before the actual samples were taken. Two samples were gathered for each sampling point, where the latter was analysed. For the rich amine sample on the TGTU, no Dopak system was available, and therefore the sample was gathered on the pressure gauge flush line for the rich amine pump. The rich MDEA and reflux water samples were collected while wearing a gas mask. All samples and their gathering points are documented according to Table 3.2.

Table 3.2: Liquid samples with names and sampling position.

Name in thesis	Sampling position
GPU lean DEA	Suction side of lean DEA pump
GPU rich DEA	Inlet of the regenerator
GPU reflux water	Reflux flow meter
TGTU lean MDEA	Absorber inlet
TGTU rich MDEA	Pressure side of the rich amine pump
TGTU reflux water	Reflux flow meter

Samples were analysed to standards according to Table 3.3. Not all samples were analysed with the same methods.

Table 3.3: List of analysis and standards used.

Analysis	Standard	GPU amine	GPU reflux	TGTU amine	TGTU reflux
pH	ISO 10523	√	√	√	√
Sulphide content	ISO 10530	√	√	√	√
Appearance	ASTM D4176	√	√	√	√
DEA-concentration	SMS 2236[a]	√	√		
MDEA-concentration	SMS 2236[a]			√	√
Density at 20°C	ISO 12185	√	√	√	√
CO_2 content	ASTM UOP829	√	√	√	√
Ammonium-content	ISO 7150-1		√		√

[a]SMS is short for Shell Method Series

pH is analysed to get a quick indicator of how much sour gases are absorbed into the amine. Appearance is another quick indicator to see if the amine is contaminated. Density of the solution at 20°C together with sulphide and carbon dioxide

concentration is used to calculate amine sour gas loadings according to Appendix A.2.2. Ammonium content for the reflux waters is measured due to the risk of side reactions between sulphides and ammonium, which can be seen as an increased measured sulphide content, higher than the amine can carry.

3.2 GPU test runs

For the GPU test runs, rich DEA, lean DEA, reflux water, sour gas and sweet gas samples were sampled and analysed. 5 test runs were done according to Table 3.4. These parameters were later modelled against. Data is averaged differently for each run to limit process disturbances.

Table 3.4: Overview of the GPU test runs.

Process parameter	**Test runs**				
	1	**2**	**3**	**4**	**5**
Date	5/2-25	26/3-25	3/4-25	8/4-25	10/4-25
Time	13:00	10:00	10:00	10:00	09:30
Time span for averaging data [min]	160	60	160	120	120
Feedstock	UCO	CFA	CFA	UCO[a]	UCO[a]
Lean amine flow to all GPU consumers [T/D]	Similiar on all test runs				
Lean amine flow to absorber [T/D]	Similiar on all test runs				
Sour gas pressure [bar(g)]	Similiar on all test runs				
Absorber pressure drop [bar]	0,14	0,11	0,12	0,15	0,15
Lean amine temp. [°C]	46,0	49,8	48,3	47,1	45,4
Sour gas temp. [°C]	32,0	31,5	32,2	32,2	32,1
Rich amine temp. [°C]	39,6	46,1	46,1	37,4	36,8
Sweet gas temp. [°C]	49,3	53,2	50,9	49,9	48,2
Regenerator top tray gas temp. [°C]	110,4	109,2	101,8	112,0	103,7
Regenerator condenser temp. [°C]	47,5	47,8	41,2	42,5	41,6

Continued on next page

Table 3.4 – continued from previous page

Process parameter	Test runs				
	1	2	3	4	5
Regenerator reflux rate/lean amine flow ratio	0,0480	0,0430	0,0213	0,0543	0,0212
Regenerator inlet temp. [°C]	99,7	101,6	100,9	99,1	97,6
Sweet gas molecular weight [g/mol]	High	Low	Low	High	High[b]
Sour gas molecular weight [g/mol]	High	Low	Low	High	High
Corrected gas flow [T/D]	Highest	Low	Low	High	High[b]
Steam to reboiler/lean amine flow ratio	0,141	0,140	0,109	0,142	0,109
Reboiler steam temp. [°C]	147,5	149,1	149,0	149,8	149,2
Reboiler steam pressure [bar(g)]	2,70	2,70	2,9	3,1	2,70
Regenerator reboiler temp. in [°C]	124,3	125,1	124,0	124,8	123,3
Amine conc. [%]	24,2	35,7	34,2	32,5	31,8

[a]Animal fat was used as part of the feed, which is similar to UCO.

[b]Molar weight calculated on Dräger analysis result instead of GC result.

3.3 TGTU test runs

For the TGTU test runs, rich MDEA, lean MDEA and reflux water were sampled and analysed. The planned test runs will be run with the following process parameters, seen in Table 3.5. Data is averaged over 2 hours before the sampling time.

Table 3.5: Overview of the TGTU test runs.

Process parameter	Test runs	
	1	2
Date	8/4-25	10/4-25
Time	10:00	10:00
Amine flow rate to absorber [T/D]	319,9	319,9
Amine flow rate to regenerator [T/D]	323,0	321,9
Regenerator condenser temp. [°C]	52,0	51,0
Regenerator inlet temp. [°C]	97,4	92,6
Lean amine temp. [°C]	38,1	27,6
Sweet gas temp. [°C]	44,2	34,5
Rich amine temp. [°C]	47,4	36,2
Gas from SCOT unit temp. [°C]	36,11	29,5
Field sour gas pressure [bar(g)]	0,3	0,3
Online sour gas pressure [bar(g)]	0,0	0,0
Pressure drop over absorber [mbar]	12,1	9,93
Reflux rate [T/D]	18,9	18,0
Regenerator bottom outlet temp. [°C]	115,9	115,3
Regenerator top temp. [°C]	107,5	107,2
Reboiler duty [kW]	804,3	812
Reboiler steam flow rate [T/D]	32,0	32,3
Reboiler steam pressure [bar(g)]	2,11	2,06
Amine concentration [%]	37,4	37,4
Absorber H_2S slip [ppm]	142	41

3.4 Model setups

3.4.1 Fluid packages and reaction sets

To simulate, HYSYS built-in functionality *Acid Gas cleaning with chemical solvents* was used. Steady state was assumed, and therefore, the property package *Equation of State* was selected for phase handling.

For reactions, HYSYS automatically generates all relevant reactions in one low temperature reaction set which is used for the absorber, and one high temperature reaction set which is used in the regenerator.

3.4.2 Tower internals and solver settings

All absorber and regenerator internals are specified according to the general arrangements supplied by St1 Refinery to represent the real columns. Since both the GPU main absorber and regenerator utilise fixed valve trays and HYSYS currently does not support the correct model of trays, the absorber has been modelled using a similar tray type, and the regenerator has been modelled by sieve trays. Both columns are specified with the same open area percentage and downcomers as the real column. The GPU flare gas absorber, which utilises random packing is modelled using metal pall rings and TGTU absorber and TGTU regenerator, which utilise structured packing, are specified according their real counterparts. The real column and model internals can be seen in Appendix C.

For column solver settings, the advanced modelling was chosen due to its rate-based approach, otherwise, HYSYS standard and recommended settings were used, except for the model trial, see Subsection 3.5. The mixed flow model was chosen due to its more robust convergence. Zhang et al. have found the flow models to have very little influence on the CO_2 absorption, and found the mixed flow model, which is the simplest, to be the closest to experimental data [42].

3.4.3 Considered components

Components considered in the GPU model, all gathered from the HYSYS built-in database, can be seen in Table 3.6

Table 3.6: Components used in the GPU amine unit simulation.

Name	HYSYS database tag	Chemical structure
Methane	Methane	CH_4
Ethane	Ethane	C_2H_6
Propane	Propane	C_3H_8
Water	H2O	H_2O
Diethanolamine	DEAmine	$HN(CH_2CH_2OH)_2$
Hexane	n-Hexane	C_6H_{14}
Isobutane	i-Butane	C_4H_{10}
Butane	n-Butane	C_4H_{10}
Carbon dioxide	CO2	CO_2
Carbon monoxide	CO	CO
Hydrogen sulphide	H2S	H_2S
Nitrogen	Nitrogen	N_2
Hydrogen	Hydrogen	H_2
i-Pentane	i-Pentane	C_5H_{12}
n-Pentane	n-Pentane	C_5H_{12}

Hexane represents all C6 hydrocarbons reported by the laboratory RGA analysis. These are important since they greatly affect the dew point of the mixture.

For the TGTU simulation, the considered components can be seen in Table 3.7

Table 3.7: Components used in the TGTU simulation.

Name	HYSYS database tag	Chemical structure
Water	H2O	H_2O
Methyldiethanolamine	MDEAmine	$CH_3N(CH_2CH_2OH)_2$
Carbon dioxide	CO2	CO_2
Hydrogen sulphide	H2S	H_2S
Nitrogen	Nitrogen	N_2
Hydrogen	Hydrogen	H_2

3.4.4 GPU amine treating model

The HYSYS GPU model has essentially all unit operations present in the real unit, excluding the lean amine surge drum, which is replaced with the makeup block and the filter setup, which is ignored. Since the model is steady state, these exclusions do not matter. In Figure 3.1, the model flowsheet can be seen.

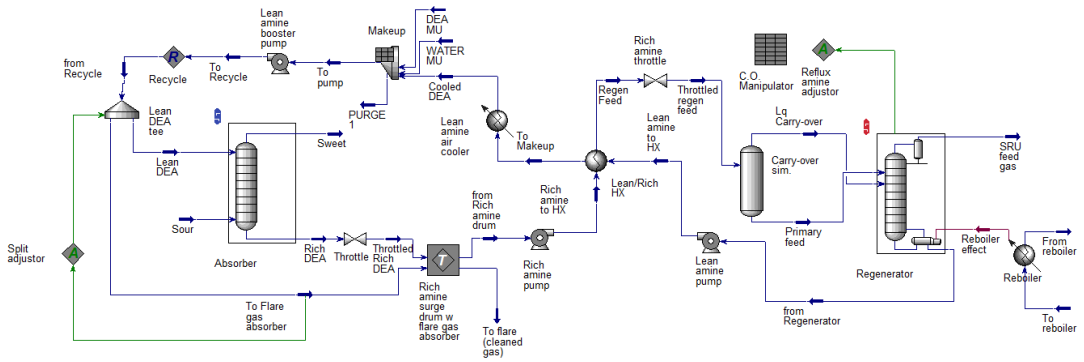

Figure 3.1: GPU model flowsheet in HYSYS, where the main parts of the model can be seen.

The GPU HYSYS model consists of the following unit operations:

3.4.4.1 Absorber

The main absorber is modelled using an absorber block, and pressures are specified by DCS readings of the HVO unit pressure. The inlet sour gas composition is specified by the experimental data from the RGA analysis. The gas flow rate is determined using a sum of all recirculation gas that enters the hydrotreating reactors and molar weight compensated according to Appendix A.3. These flows are compared to flows calculated from mass balances in section 5.

3.4.4.2 Rich amine surge drum with flare gas absorber

The rich amine surge drum doubles as a flash separator, separating the lighter fractions that have evaporated after throttling to 1 bar(g). The drum has a small absorber on top, which cleans out additional sour gases to not send sour gases onto the flare system. The amine feed to this absorber is set by a manual control valve to approximately 0,25 m^3/h, which is very small compared to the main amine circulating flow. The outlet from the absorber and the rich amine surge drum are merged in a tee, which is jointly sent towards the rich amine pump. The submodel setup can be seen in Figure 3.2.

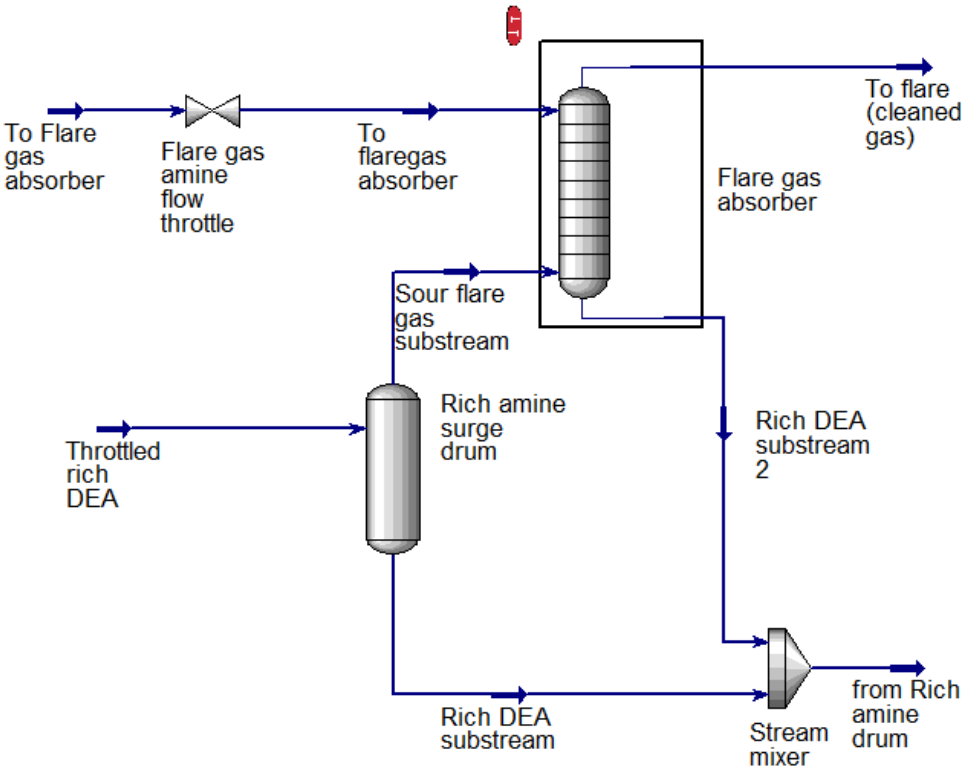

Figure 3.2: GPU rich amine surge drum with flare gas absorber sub-model in HYSYS.

In the real unit, the absorber is mounted directly on top of the surge drum, and the lean DEA is mixed directly in the drum.

3.4.4.3 Lean/rich heat exchanger

The lean/rich heat exchanger is modelled by using a heat exchanger with no pressure drop, and the temperature is specified according to DCS readings for the regenerator feed.

3.4.4.4 Amine regenerator

Amine regenerator was modelled using a full reflux distillation column, specified by reboiler duty and condenser temperature. The reflux drum pressure and condenser temperature were set to 0,9 bar(g) for all test runs, since the DCS value was the same for all experiments. The bottom pressure was adjusted after bottom temperature readings, since no accurate pressure readings could be gathered, the adjusted pressure was however, verified using a manual pressure gauge fitted under tray 1 on site. The reboiler is of kettle type fed by medium-pressure steam, and the steam data is specified by DCS readings, assuming the outlet steam is considered fully condensed.

To model amine carry-over, a separator was put in line with the feed, after the throttle. This separator utilised a feed-based carry-over model, where a speci-

fied fraction of the liquid feed was carried by the gaseous phase. The separator vapour outlet was led straight to the distillation columns' condenser. This was recommended by AspenTech's support team after being consulted. The liquid outlet was led to the same tray as the normal feed. Carry over is only modelled for the complete system, since no residual gases are dissolved in the feed for the solo models.

3.4.4.5 Lean amine air cooler

This air cooler is represented by a cooler block, with a specified outlet temperature read from the DCS.

3.4.4.6 Makeup block and recycle

The makeup block represents the lean amine surge drum, but only functions as amine and water makeup, and the recycle block closes the loop. The makeup is handled differently on the real unit, where both concentrated DEA solution and water is added on irregular basis by operators.

3.4.5 TGTU model

The TGTU unit can be considered a simpler version of the GPU unit, where the main differences are the following:

1. Smaller unit with a different objective
2. Utilizes MDEA instead of DEA as its solvent
3. Much lower pressure in the absorber, slightly lower pressure in the regenerator
4. No rich amine drum
5. Wildly different sour gas inlet flow and composition.
6. No easy way of measuring gas composition in and out of the absorber

The model setup can be seen in Figure 3.3. The TGTU unit is only run as a complete model with both absorber and regenerator.

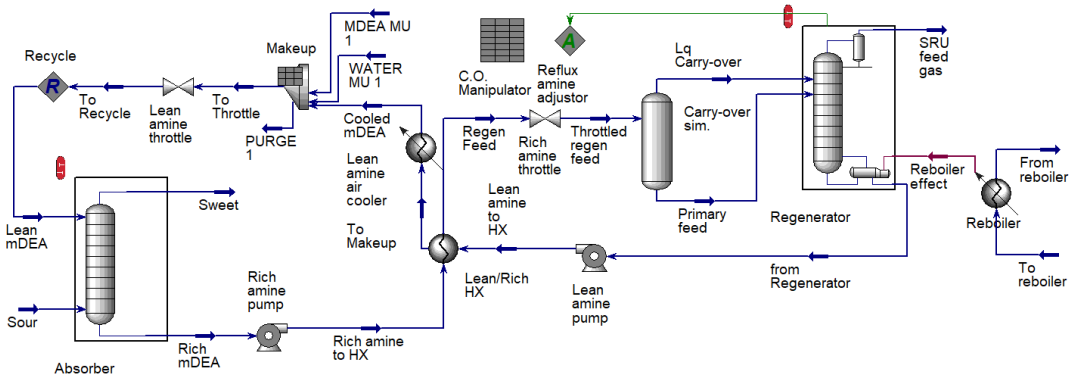

Figure 3.3: TGTU model setup in HYSYS, where the main parts of the model can be seen.

3.4.5.1 Absorber

The TGTU absorber is modelled using an absorber block. The inlet temperature is taken from the DCS. The pressure is read on a manual gauge in the field, but were 0,3 bar(g) at both runs.

To estimate the flow onto the TGTU absorber, an iterated mass balance based on numerous quality instruments and Coriolis flow meters is needed. The relevant instruments and unit structure can be seen in Figure 3.4.

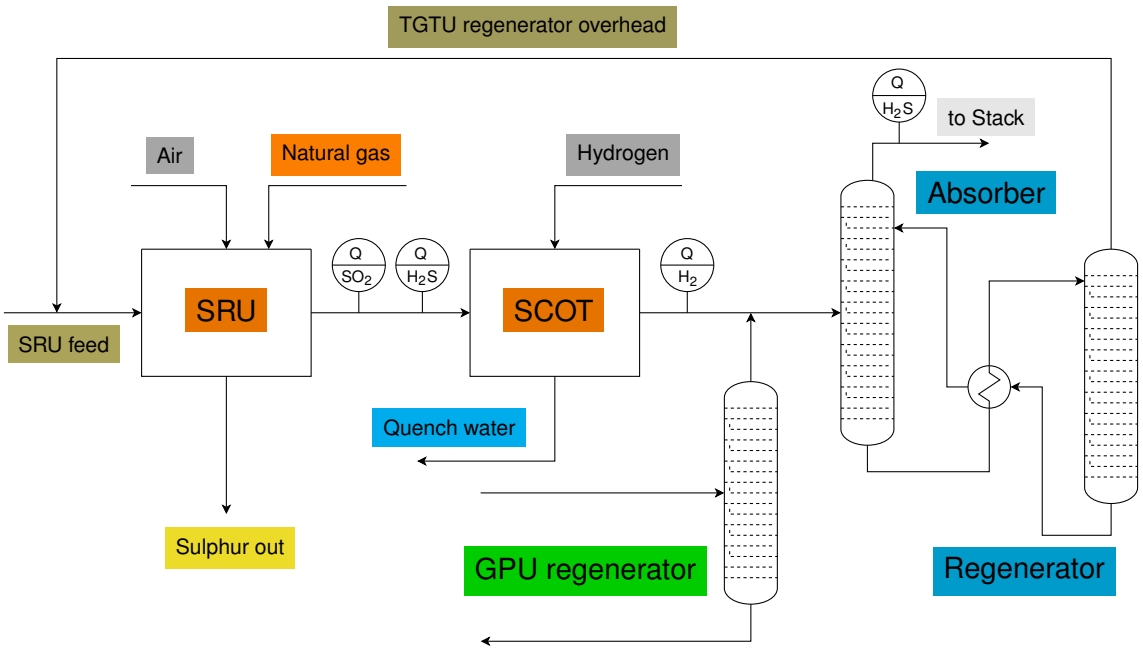

Figure 3.4: Process flow diagram of the different streams used for the mass balance around the TGTU.

The mass balance consists of a few parts. First, the natural gas flow onto the SRU main furnace is taken from a Coriolis flow meter. This gas comes from the Nordic

natural gas grid, and its carbon content is analysed monthly by the grid operator, Swedegas [43]. Anything other than carbon is assumed to be hydrogen. With this, the CO_2 and H_2O produced by combustion and the O_2 needed for full combustion can be determined. From the O_2 need, the corresponding nitrogen gas flow into the unit can be calculated.

Second, analysis of feed and product sulphur contents from the refinery hydrotreating units is gathered. Multiplied by the unit's feed rate, it is possible to estimate how much sulphur is fed to the SRU and therefore iterate how much oxygen demand there is to achieve a certain H_2S conversion in the unit. In addition to this, it is possible to verify the estimated sulphur amounts from the hydrotreating units with the amounts fed to the sulphur storage tank. This is further described in Appendix E. Added to this, the TGTU regenerator overhead is led back to the SRU feed, and this stream of CO_2 was calculated from the amine experimental results and H_2S were estimated from the total sulphur formed in the SRU together with how much H_2S is fed from the GPU regenerator overhead.

Conversion in the SRU is dependent on the feed rate of H_2S and how much natural gas is fired, a lower H_2S rate requires higher natural gas firing to get sufficient temperature, but does require a higher air flow onto the main conversion furnace. Therefore, a conservative 90% H_2S conversion rate was assumed. Both SO_2 and H_2S slip from the SRU are measured using online quality instruments and can be verified against the mass balance.

Third, the SRU output stream is fed to a Shell Claus Off-gas treating (SCOT) unit. This unit converts nearly 100% of SO_2 into H_2S with added H_2. The added H_2 is measured with a Coriolis flow meter, and its hydrogen content is sampled at regular intervals, often at a quality of around 90% H_2 content. After the reactor, the SCOT unit has a quench tower which condenses close to all H_2O that comes from natural gas combustion. At the top of the quench tower, hydrogen slip from the SCOT reactor is measured with an online quality instrument. This makes it possible to iterate a mass flow out from the SCOT unit by adjusting how much water and hydrogen gases are entrained from the quench tower.

Fourth, the SCOT output gas is mixed with the GPU regenerator overhead, which is calculated from the GPU test runs. To measure how much CO_2 and H_2S are picked up in the TGTU absorber, a mass balance over the amine can be calculated. There is an online quality instrument that measures H_2S slip on the absorber gas outlet stream to compare the calculated values to.

The calculated results from the mass balances can be seen in Table 3.8:

Table 3.8: Calculated values from TGTU mass balance.

Process parameter	Test runs	
	1	2
Date	8/4-25	10/4-25
H_2S fed to SRU unit [T/D][a]	1,59	1,85
Total gas flow to absorber [kmol/day]	1211,2	1177,03
CO_2 in absorber inlet [mol%]	37,07	35,51
H_2S in absorber inlet [mol%]	2,45	1,82
Inert gasses in absorber inlet [mol%]	56,39	58,82
H_2 in absorber inlet [mol%]	4,09	3,85
Molecular weight [g/mol]	33,03	32,80

[a] Verified against tank levels according to Appendix E.

A third TGTU test run was planned and conducted with a high feed rate of H_2S to the SRU, where sulphur produced were approximated to 6,5 T/D. However, due to considerable uncertainty in the mass balance, it was decided not to use this data in the analysis.

3.4.5.2 Regenerator

The TGTU regenerator is modelled in the same way as for the GPU regenerator, see Subsubsection 3.4.4.4. The main differences, apart from the size and internals, are the lower pressure and that the reboiler is fed with low-pressure steam. The reflux drum pressure and condenser temperature were set to 0,3 bar(g) for both test runs.

3.5 Model parameter study

A model parameter study will be carried out according to a full factorial experimental setup, which will test out different tray and mass transfer models for the absorber and regenerator. For the absorber, the Koch, and Nutter valve tray models will be compared with either AIChE, Gerster or Scheffe mass transfer models. The regenerator will be tested with either sieve trays or Nutter valve trays. The valve trays will be compared with the same mass transfer models as for the absorber, and for the sieve trays will be compared with Chan-Fair, Chan-Fair-RF (RateFrac), Gerster, Chen-Chuang or AIChE. A full factorial experiment setup with results can be seen in Appendix D. The model parameter study is based on GPU test run 2.

4

Results

In this chapter, the results from the experimental runs will be presented, and afterwards, the model results will be compared to the experimental results.

4.1 GPU experimental runs

In this section, results from the GPU experimental runs will be presented, and anomalies will be highlighted.

4.1.1 Results 1:

In Table 4.1 results from the first GPU test run can be seen. Both the regenerator and the absorber perform well.

Table 4.1: Results from GPU run 1:

GPU run 1: RGA 1	**Sour gas**	**Sweet gas**	**Reduction**
CO_2 Dräger (ml/m^3)			-90,0%
H_2S Dräger (ml/m^3)		<0,2	
CO_2 GC (mol%)			-89,0%
H_2S GC (mol%)	<0,1	<0,1	-
	Rich DEA	**Lean DEA**	**Reduction**
DEA (wt%)	-	24,2	-
Density (kg/m^3)	1065,2	1031,4	-
Sulphide concentration (g/l)	2,24	0,071	-
CO_2 concentration (g/l)	29,57	1,33	-
H_2S loading (mol_{H_2S}/mol_{DEA})	0,0293	0,000932	-96,8%
CO_2 loading (mol_{CO_2}/mol_{DEA})	0,282	0,0127	-95,5%

[a]Reproducibility from RGA 1 analysis were poor.

In Table 4.2 results from analysing the reflux water from test run 1 can be seen. The DEA content is high for a reflux water and signifies that some carry-over

is occurring in the regenerator. No CO_2 loading for the reflux water could be calculated for this run, since the analysis was not carried out.

Table 4.2: Results from reflux sample in GPU run 1:

GPU run 1	**Regenerator reflux**
DEA (wt%)	6,8
Density (kg/m^3)	1021,1
Sulphide concentration (g/l)	1,37
CO_2 concentration (g/l)	-
H_2S loading (mol_{CO_2}/mol_{DEA})	0,0635
CO_2 loading (mol_{H_2S}/mol_{DEA})	-
Ammonium concentration (mg/l)	0,3

4.1.2 Results 2:

In Table 4.3 results from the second GPU test run can be seen. The H_2S slip is higher in this run compared to the other runs. The regenerator performs well. Lean amine had a persistent foam on it when sampled.

Table 4.3: Results from GPU run 2:

GPU run 2: RGA 1	**Sour gas**	**Sweet gas**	**Reduction**
CO_2 Dräger (ml/m^3)			-93,3%
H_2S Dräger (ml/m^3)		4	
CO_2 GC (mol%)	[a]	[a]	-88,8%
H_2S GC (mol%)	<0,1	<0,1	-
	Rich DEA	**Lean DEA**	**Reduction**
DEA (wt%)	-	35,7	-
Density (kg/m^3)	1082,6	1047,5	-
Sulphide concentration (g/l)	1,84	0,074	-
CO_2 concentration (g/l)	36,69	1,85	-
H_2S loading (mol_{H_2S}/mol_{DEA})	0,020	0,00065	-96,7%
CO_2 loading (mol_{CO_2}/mol_{DEA})	0,234	0,0118	-95,0%

[a]Reproducibility from RGA 1 analysis were poor.

In Table 4.4, results from analysing the reflux water from test run 2 can be seen. The DEA content is high for a reflux water and signifies that some carry-over is occurring in the regenerator. Ammonium concentration is extreme and highlights some problems with either the unit or the method of analysis.

Table 4.4: Results from reflux sample in GPU run 2:

GPU run 2	**Regenerator reflux**
DEA (wt%)	3,6
Density (kg/m^3)	1011,2
Sulphide concentration (g/l)	0,975
CO_2 concentration (g/l)	13,79
H_2S loading (mol_{H_2S}/mol_{DEA})	0,0881
CO_2 loading (mol_{CO_2}/mol_{DEA})	0,9082
Ammonium concentration (mg/l)	7480

4.1.3 Results 3:

In Table 4.5 results from the third GPU test run can be seen. This test run has the highest absorber CO_2 removal.

Table 4.5: Results from GPU run 3:

GPU run 3: RGA 2	**Sour gas**	**Sweet gas**	**Reduction**
CO_2 Dräger (ml/m^3)			-94,0%
H_2S Dräger (ml/m^3)		1	
CO_2 GC (mol%)			-92,3%
H_2S GC (mol%)	<0,1	<0,1	-
	Rich DEA	**Lean DEA**	**Reduction**
DEA (wt%)	-	34,2	-
Density (kg/m^3)	1080,2	1046	-
Sulphide concentration (g/l)	2,40	0,268	-
CO_2 concentration (g/l)	38,36	3,45	-
H_2S loading (mol_{H_2S}/mol_{DEA})	0,0220	0,00246	-88,8%
CO_2 loading (mol_{CO_2}/mol_{DEA})	0,257	0,0231	-91,0%

In Table 4.6, results from analysing the reflux water from test run 3 can be seen. Ammonium concentration is high.

Table 4.6: Results from reflux sample in GPU run 3:

GPU run 3	Regenerator reflux
DEA (wt%)	1,44
Density (kg/m^3)	1003,7
Sulphide concentration (g/l)	0,488
CO_2 concentration (g/l)	6,34
H_2S loading (mol_{H_2S}/mol_{DEA})	0,111
CO_2 loading (mol_{CO_2}/mol_{DEA})	1,05
Ammonium concentration (mg/l)	2290

4.1.4 Results 4:

In Table 4.7 results from the fourth GPU test run can be seen. This test run has one of the lowest absorber CO_2 removals. The regenerator performance is good. Lean amine had a persistent foam on it when sampled.

Table 4.7: Results from GPU run 4:

GPU run 4: RGA 2	**Sour gas**	**Sweet gas**	**Reduction**
CO_2 Dräger (ml/m^3)			-94,0%
H_2S Dräger (ml/m^3)		1	
CO_2 GC (mol%)		[a]	-85,5%
H_2S GC (mol%)	<0,1	<0,1	-
	Rich DEA	**Lean DEA**	**Reduction**
DEA (wt%)	-	32,54	-
Density (kg/m^3)	1070,9	1043	-
Sulphide concentration (g/l)	1,91	0,085	-
CO_2 concentration (g/l)	30,30	1,67	-
H_2S loading (mol_{H_2S}/mol_{DEA})	0,018	0,00082	-95,5%
CO_2 loading (mol_{CO_2}/mol_{DEA})	0,214	0,0118	-94,5%

[a] 1 of 3 replicates had slightly lower reproducibility.

In Table 4.8, results from analysing the reflux water from test run 4 can be seen. Ammonium concentration is extremely high. DEA concentration is very high, which signifies high carry-over.

Table 4.8: Results from reflux sample in GPU run 4:

GPU run 4: RGA 2	**Regenerator reflux**
DEA (wt%)	11,21
Density (kg/m^3)	1034,4
Sulphide concentration (g/l)	3,5
CO_2 concentration (g/l)	39,14
H_2S loading (mol_{H_2S}/mol_{DEA})	0,10
CO_2 loading (mol_{CO_2}/mol_{DEA})	0,8410
Ammonium concentration (mg/l)	23320

4.1.5 Results 5:

In Table 4.9 results from the fifth GPU test run can be seen. This test run has the lowest absorber CO_2 removal where the dräger tube and GC diverge, which questions the validity of the GC analysis. The laboratory engineer reported consistency problems with the equipment, which, according to the standard, analyses the gases with a multipla of sensors. No consistency error on hydrocarbon composition was reported, which is detected by a flame ionisation detector (FID), but the time-of-flight (TOF) detector, which detects CO_2, reported different values each run. This GC analysis point is therefore excluded when discussing the compiled results. The regenerator performance is lower than on the other runs.

Table 4.9: Results from GPU run 5:

GPU run 5: RGA 1	**Sour gas**	**Sweet gas**	**Reduction**
CO_2 Dräger (ml/m^3)			-90,0%
H_2S Dräger (ml/m^3)		1	
CO_2 GC (mol%)	[a]	[a]	-41,7%
H_2S GC (mol%)	<0,1	<0,1	-
	Rich DEA	**Lean DEA**	**Reduction**
DEA (wt%)	-	31,83	-
Density (kg/m^3)	1068,7	1042,5	-
Sulphide concentration (g/l)	1,33	0,162	-
CO_2 concentration (g/l)	28,35	2,78	-
H_2S loading (mol_{H_2S}/mol_{DEA})	0,0131	0,00160	-87,8%
CO_2 loading (mol_{CO_2}/mol_{DEA})	0,204	0,0200	-90,2%

[a]Reproducibility from RGA 1 analysis were poor.

In Table 4.10, results from analysing the reflux water from test run 5 can be seen. Ammonium concentration is extremely high. DEA concentration is very high, which signifies high carry-over.

Table 4.10: Results from reflux sample in GPU run 5:

GPU run 5	**Regenerator reflux**
DEA (wt%)	8,67
Density (kg/m^3)	1028,4
Sulphide concentration (g/l)	2,36
CO_2 concentration (g/l)	34,24
H_2S loading (mol_{H_2S}/mol_{DEA})	0,0876
CO_2 loading (mol_{CO_2}/mol_{DEA})	0,9257
Ammonium concentration (mg/l)	15040

4.2 Compiled GPU experimental and model results

4.2.1 Absorber and regenerator model results

In Figure 4.1, the absorber model result can be compared against the experimental plant data. The model seems to capture the differences between runs; however, at runs with lower CO_2 removal, the model seems to overpredict performance. For H_2S, the model seems to have trouble capturing differences between runs; however, this is for very small concentrations, and the accuracy is low in the analysis.

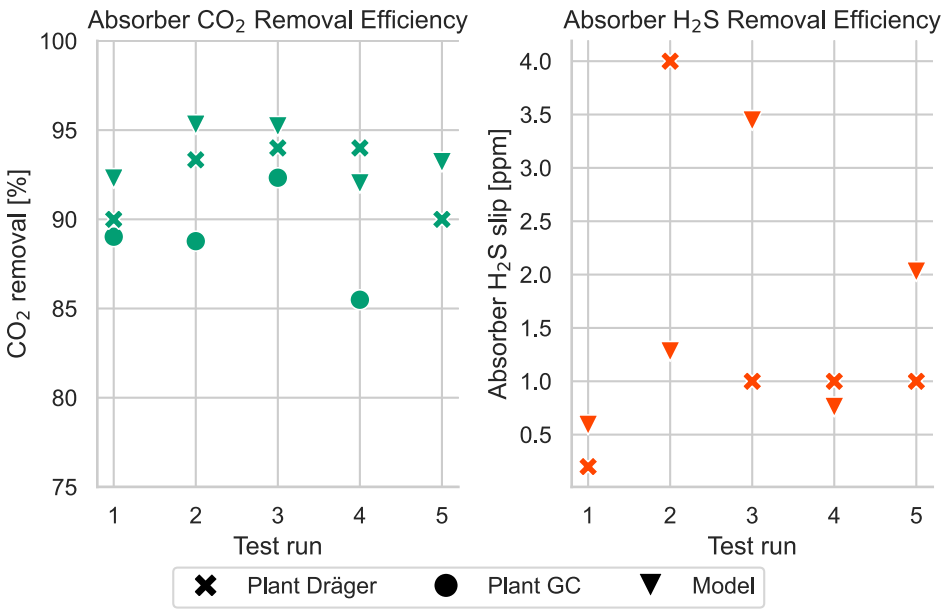

Figure 4.1: Absorber efficiency, plant and model results plotted over the test runs.

In Figure 4.2, the regenerator model result can be compared against the experimental plant data. For CO_2, the model captures differences well, but for H_2S, the lean amine is constantly loaded higher than the model predicts.

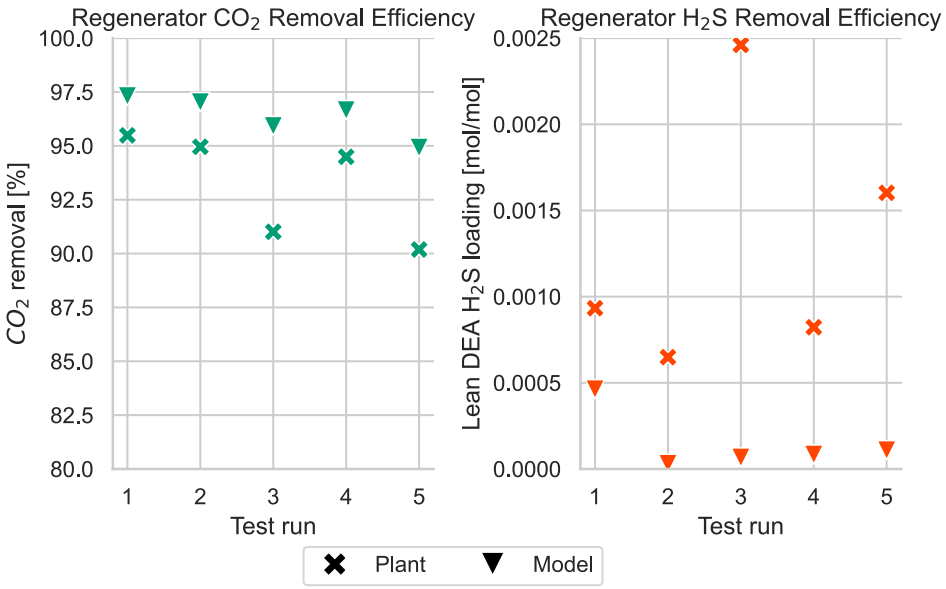

Figure 4.2: Regenerator efficiency, plant and model results plotted over the test runs.

4.2.2 Complete amine system model results

In Figure 4.3, the absorber CO_2 removal and H_2S slip are plotted for both the experimental and complete system model results. The results look similar to the solo absorber models, but differences are exaggerated.

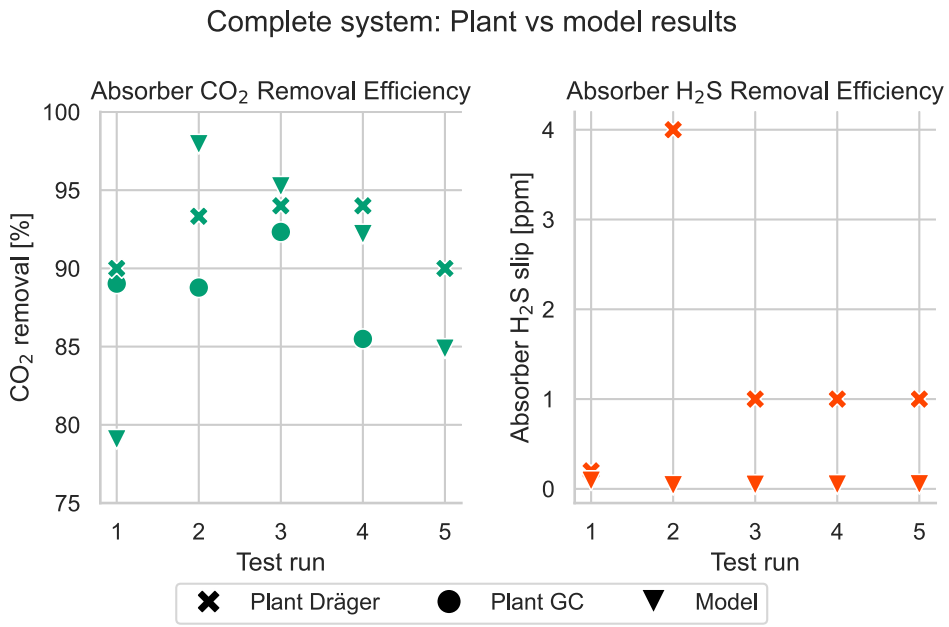

Figure 4.3: Absorber efficiency for the complete system, plant and model results plotted over the test runs.

In Figure 4.4, the regenerator CO_2 removal and lean amine H_2S loading are plotted for both the experimental and model results. The regenerator performs similarly in the complete system as in the solo regenerator models.

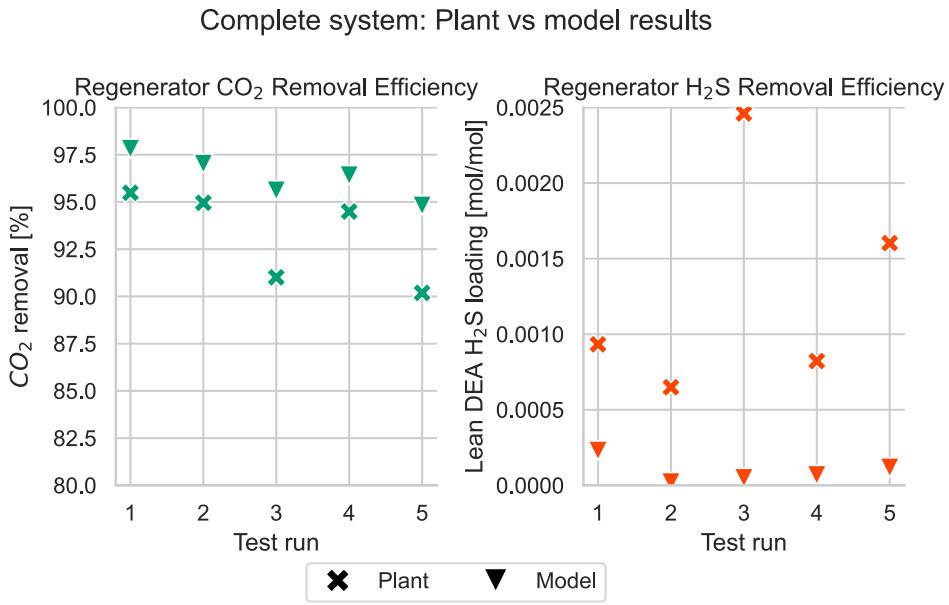

Figure 4.4: Complete system: Regenerator efficiency, Plant vs model.

It is clear that the model does seem to be able to capture differences between the runs, but consistently overpredicts performance. This could be due to either

the absorber or the regenerator overperforming leading to the other one overperforming. The results highlights that there is problems with the units and that they do not function ideally.

4.3 GPU operating parameter study

In this section, GPU experimental and model results will first be compared to the amine concentration and later reboiler duty.

4.3.1 Amine concentration

In Figure 4.5, amine concentration from the runs and models is plotted against CO_2 removal and H_2S slip for the absorber. For CO_2, there is no clear trend between the experimental and model results, and they diverge. Therefore, it is uncertain if a higher amine concentration yields a higher CO_2 removal. For H_2S, the model predicts lower slip for higher amine concentrations, but experimental results show no clear correlation, since most results are gathered around 1 ppm.

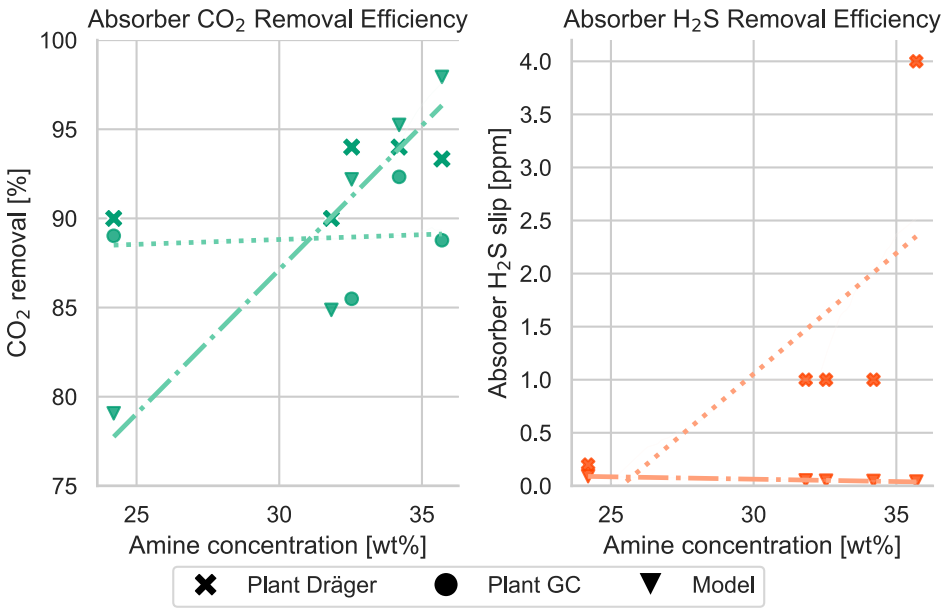

Figure 4.5: CO_2 removal and H_2S slip for the absorber plotted against amine concentration. Dotted lines are regression trends for GPU GC analysis and GPU H2S analysis. Mixed lines are regression lines for model predictions.

In Figure 4.6 amine concentration from the runs and models is plotted against CO_2 removal and lean DEA H_2S loading for the regenerator. Both the model and experimental results show a slight decline in regenerator CO_2 removal at higher amine concentrations. For H_2S, the model predicts lower loadings for higher concentrations, but the results from experimental runs show no clear correlations. To be noted, this is very low concentrations.

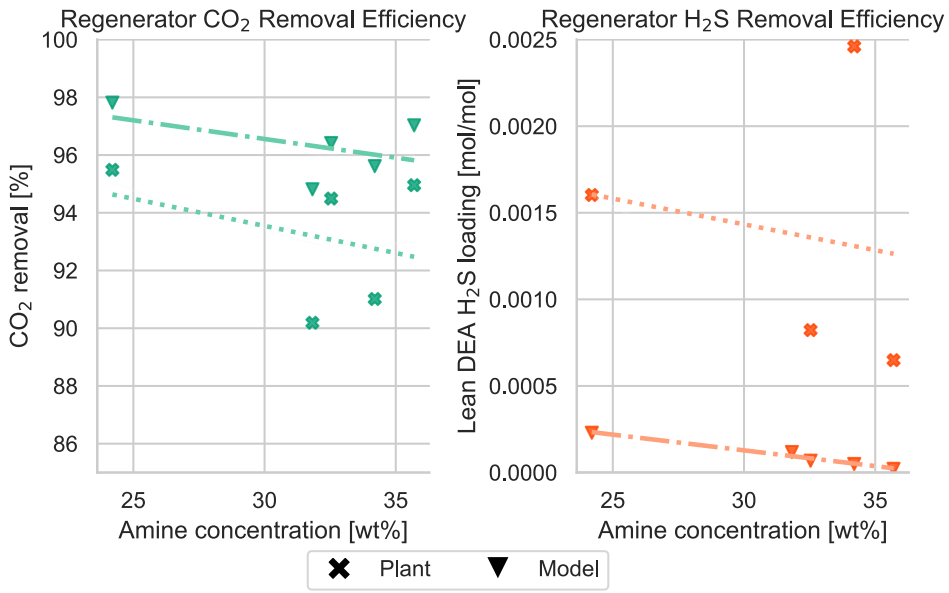

Figure 4.6: CO_2 removal and lean DEA H_2S loading for the regenerator plotted against amine concentration. Dotted lines are regression trends for experimental results. Mixed lines are regression lines for model predictions.

It can be stated that amine concentration has relatively little impact on the regenerator. To further prove this, more runs with lower concentrations may be necessary. In Figure 4.7, a sensitivity analysis on amine concentration for the absorber in test run 4 can be seen. It indicates that the H_2S slip is kept low (under 1 ppm) over the concentration span, but CO_2 absorption varies heavily. The study indicates that higher concentrations always yield lower slip and higher CO_2 removal. This is not in line with the experimental results, which may show that it is not as simple as that.

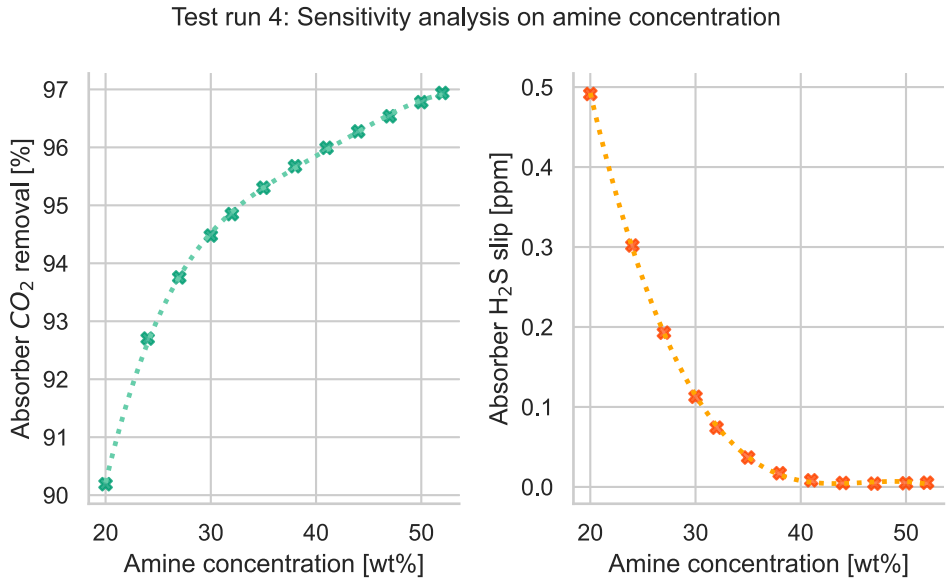

Figure 4.7: Sensitivity study on Test run 4 where amine concentration is changed.

4.3.2 Reboiler duty

In Figure 4.8, ratio between steam flow rate and lean amine flow rate in the regenerator from the runs and models is plotted against CO_2 removal and H_2S slip for the absorber. The results from both experiments show that a lower reboiler duty yields higher CO_2 absorption. For H_2S slip, the results are scattered and show no clear trends. The models show that the reboiler duty has little to no impact on absorber performance.

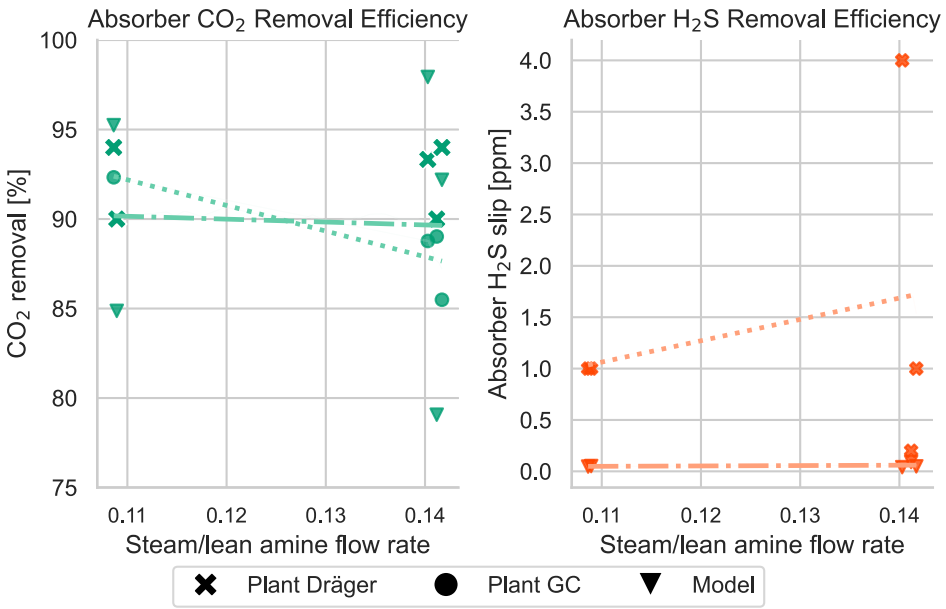

Figure 4.8: CO_2 removal and H_2S slip for the absorber plotted against ratio between steam flow rate and lean amine flow rate. Dotted lines are regression trends for GPU GC analysis and GPU H2S analysis. Mixed lines are regression lines for model predictions.

In Figure 4.9, ratio between steam flow rate and lean amine flow rate from the runs and models is plotted against CO_2 removal and lean DEA H_2S loading for the regenerator. Both models and experiments show that a higher steam/lean ratio results in more CO_2 being stripped out. For H_2S, the amine is minimally loaded already at the lower reboiler duty, therefore, very little will happen when increasing the steam flow rate.

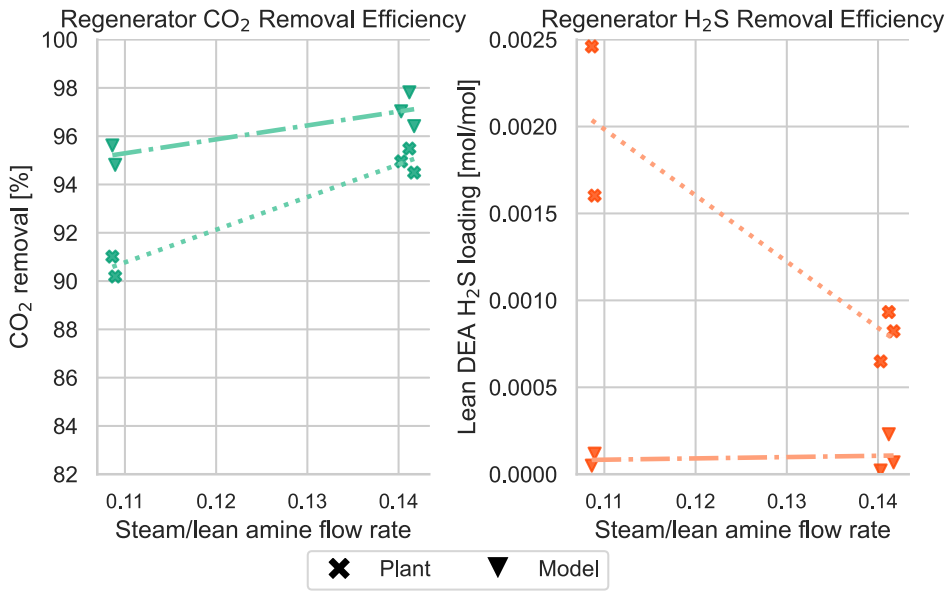

Figure 4.9: CO_2 removal and lean DEA H_2S loading for the regenerator plotted against ratio between steam flow rate and lean amine flow rate. Dotted lines are regression trends for experimental results. Mixed lines are regression lines for model predictions.

4.4 Amine flow rate

This sensitivity analysis is based on the model for GPU experimental run 5. In Figure 4.10 and 4.11, the steam flow rate is kept constant and the amine flow rate is varied. This results in a varying steam flow rate/lean amine flow rate ratio between 0.08 to 0.144, and absorber and regenerator performance can be seen. Since the reboiler duty is constantly set to for this analysis, both the CO_2 removal decreases and lean amine H_2S loading increases with higher flows. H_2S is, however, less affected than CO_2 as the decrease seems to be milder. For the absorber, the optimum for H_2S absorption is found at a lower amine flow rate than for CO_2. H_2S slip starts to increase at larger flows, but CO_2 absorption only increases.

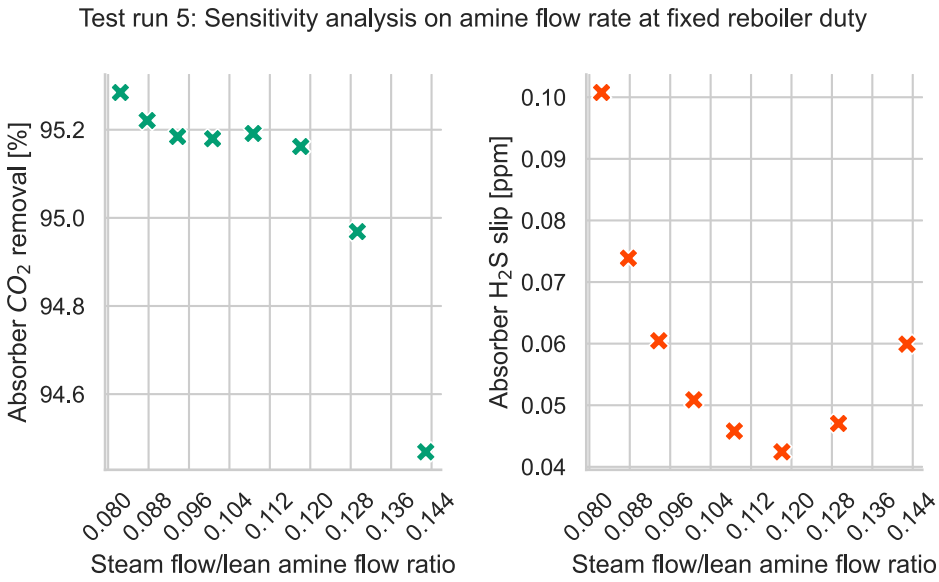

Figure 4.10: Simulated amine flow rate changes based on GPU test run 5 plotted against absorber CO_2 removal and H_2S slip at fixed reboiler duty.

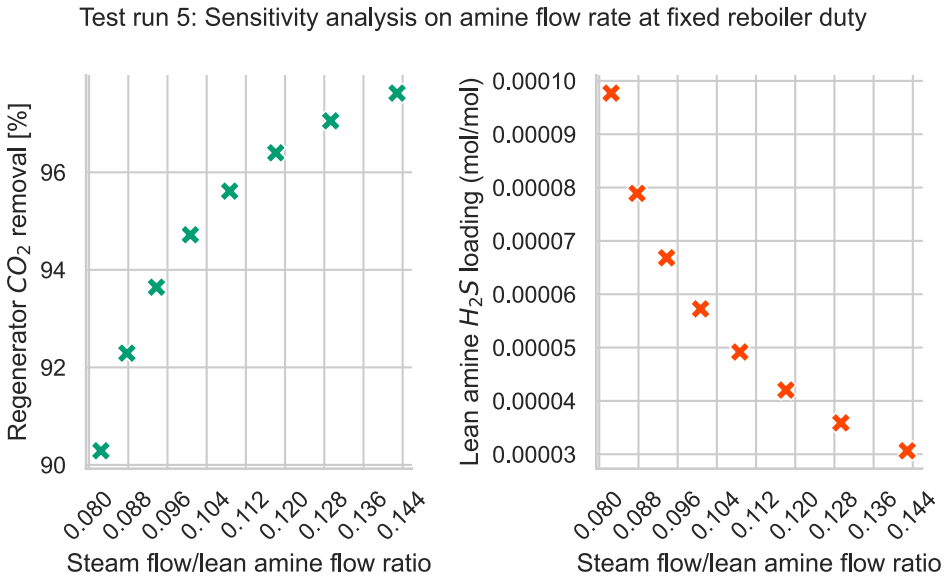

Figure 4.11: Simulated amine flow rate changes based on GPU test run 5 plotted against regenerator CO_2 removal and lean amine H_2S loading at fixed reboiler duty.

4.5 TGTU test runs

In this section, results from the TGTU test runs are presented and evaluated.

4.5.1 Results 1:

In Table 4.11, results from the first TGTU test run can be seen. Heavy green tint on rich amine, which couldn't be analysed by the spectroscopic method that is used for sulphide concentration. Green tint could be an indicator of iron sulphide (FeS) contamination [44]. The regenerator seems to have problems stripping off CO_2.

Table 4.11: Results from TGTU run 1:

TGTU run 1	Rich MDEA	Lean MDEA	Reduction
MDEA (wt%)	-	37,43	-
Density (kg/m^3)	1086,4	1065,5	-
Sulphide concentration (g/l)	-	-	-
CO_2 concentration (g/l)	50,59	31,13	-
H_2S loading (mol_{CO_2}/mol_{MDEA})	-	-	-
CO_2 loading (mol_{H_2S}/mol_{MDEA})	0,3411	0,2043	-40,09%

In Table 4.12, analysis results for the reflux water are presented. A higher-than-normal amine content is reported, which indicates that the regenerator is suffering from carry-over. Ammonium content is very high.

Table 4.12: Results from reflux sample in TGTU run 1:

TGTU run 1	Regenerator reflux
MDEA (wt%)	3,68
Density (kg/m^3)	1007,4
Sulphide concentration (g/l)	3,61
CO_2 concentration (g/l)	11,34
H_2S loading (mol_{CO_2}/mol_{MDEA})	0,364
CO_2 loading (mol_{H_2S}/mol_{MDEA})	0,8346
Ammonium concentration (mg/l)	5740

4.5.2 Results 2:

In Table 4.13, results from the second TGTU test run can be seen. Similar to the second test run, a heavy green tint on rich amine is noted. The regenerator has problems with stripping out CO_2.

Table 4.13: Results from TGTU run 2:

TGTU run 2	Rich MDEA	Lean MDEA	Reduction
MDEA (wt%)	-	37,38	-
Density (kg/m^3)	1083	1066,7	-
Sulphide concentration (g/l)	-	-	-
CO_2 concentration (g/l)	43,92	31,57	-
H_2S loading (mol_{CO_2}/mol_{MDEA})	-	-	-
CO_2 loading (mol_{H_2S}/mol_{MDEA})	0,2947	0,2072	-29,69 %

In Table 4.14 analysis results for the reflux water are presented. A higher-than-normal amine content is reported, which indicates that the regenerator is suffering from carry-over. Ammonium content is very high.

Table 4.14: Results from reflux sample in TGTU run 2:

TGTU run 2	Regenerator reflux
MDEA (wt%)	4,21
Density (kg/m^3)	1008,6
Sulphide concentration (g/l)	3,78
CO_2 concentration (g/l)	13,34
H_2S loading (mol_{CO_2}/mol_{MDEA})	0,334
CO_2 loading (mol_{H_2S}/mol_{MDEA})	0,8583
Ammonium concentration (mg/l)	5280

4.6 Compiled TGTU experimental and model results

In Figure 4.12, compiled results from TGTU test runs and modelling can be seen. It is visible that the real absorber absorbs a lot more CO_2 than the model absorber. This could explain the higher amounts of H_2S slip that are reported. For test run 2, the modelled H_2S slip is the same as the test run result, but absorption of CO_2 is still way higher than the model predicts.

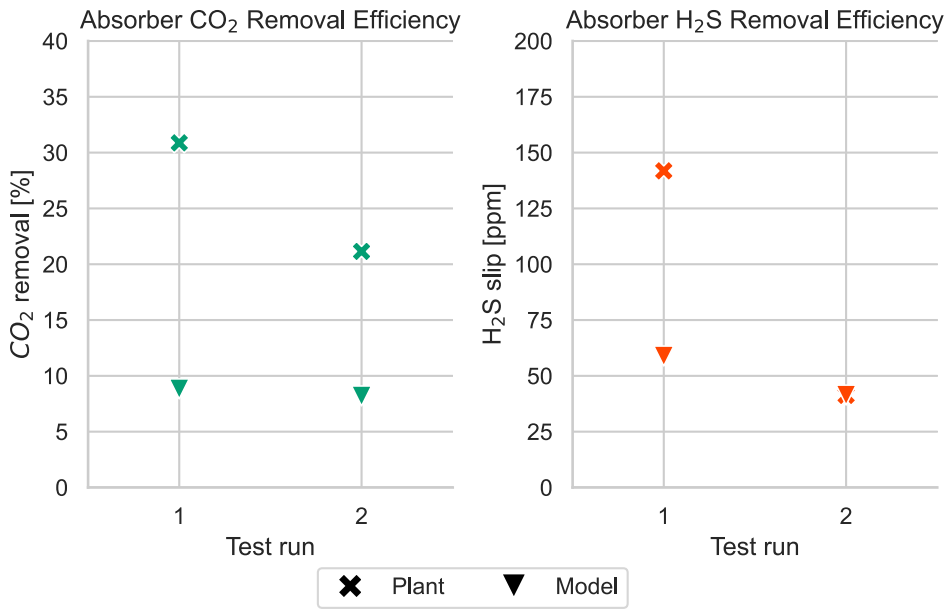

Figure 4.12: Absorber efficiency, TGTU vs model.

In Figure 4.13, results from TGTU test runs and models can be compared. They differ to a very high extent, which indicates that the model clearly cannot predict the regenerator at its current malfunctioning state.

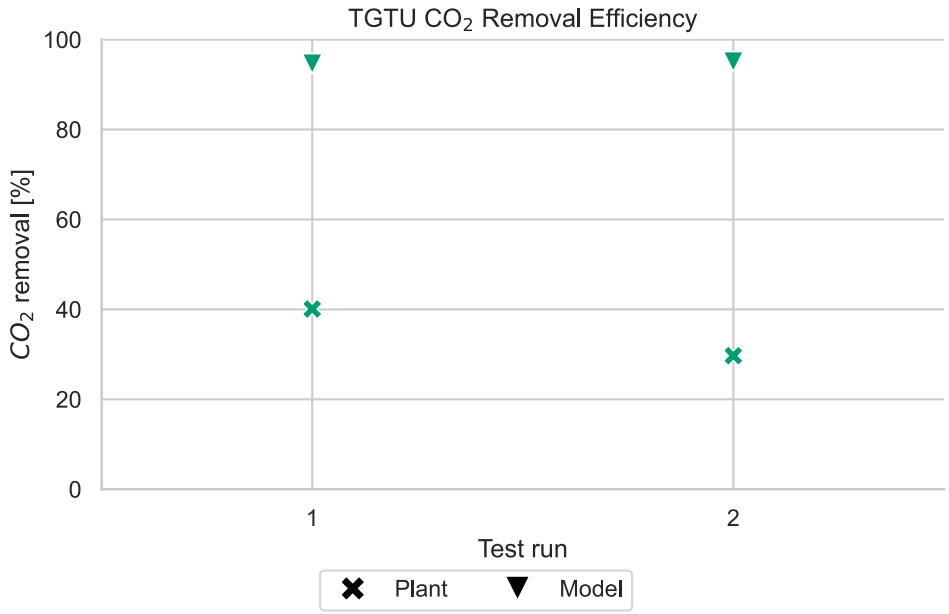

Figure 4.13: Regenerator efficiency, TGTU vs model.

4.6.1 Sensitivity analysis of TGTU amine concentration

In Figure 4.14, a sensitivity analysis on amine concentration based on test run 2 can be seen. The analysis indicates that higher concentrations of amine decrease

CO_2 absorption but do increase H_2S slip, however, the effect is minor.

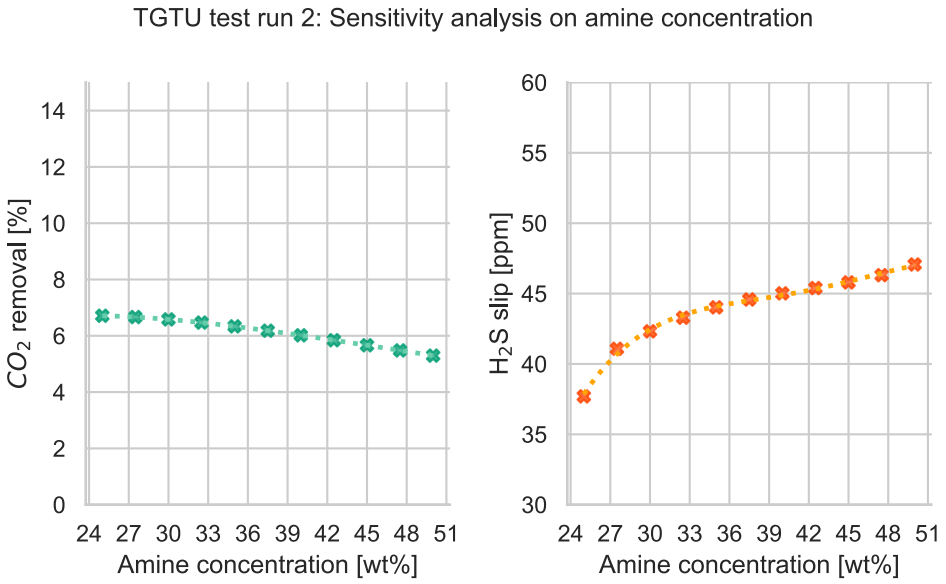

Figure 4.14: Sensitivity analysis on amine concentration for TGTU.

This may look wrong at first glance, but since the difference is tiny, this could probably be explained by mass transfer effects. Higher concentrations of MDEA yield higher viscosity, which generally lowers mass transfer in columns. In Figure 4.15, viscosity is plotted against total rich amine acid gas loading.

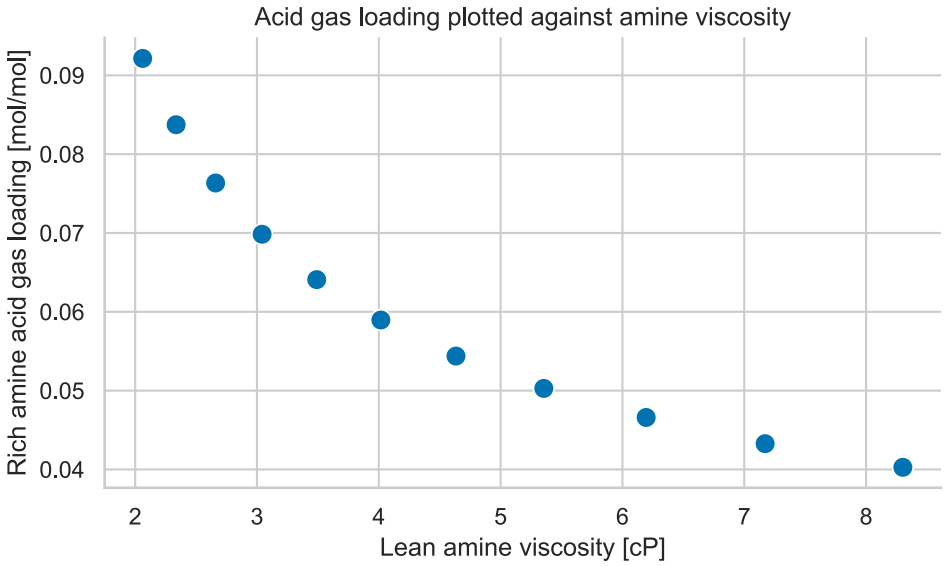

Figure 4.15: Viscosity of the rich amine plotted against he acid gas loading of the rich amine. Viscosity decreases when the acid gas loading decreases.

4.7 Results from model parameter study

In this section, the results from the model parameter study will be presented. In Figure 4.16, it can be seen that CO_2 removal differs by a few per cent units between the different tests. Run 32, where the highest removal is observed, comes from a model combination where the Nutter tray model is used for the absorber and the sieve model is used in the regenerator together with AIChE as the mass transfer model for both. Lowest removal in tests 22, 23, 47, and 48 is from using the sieve model with Chen-Chuang mass transfer model in the regenerator, together with either of the combinations in the absorber. Test 1 to 24 utilize the Koch tray model and test 25 to 48 utilize the Nutter model. There is little difference between the Nutter and the Koch tray models for the absorber. The Scheffe tray model predicts better performance than both the Gerster and the AIChE models.

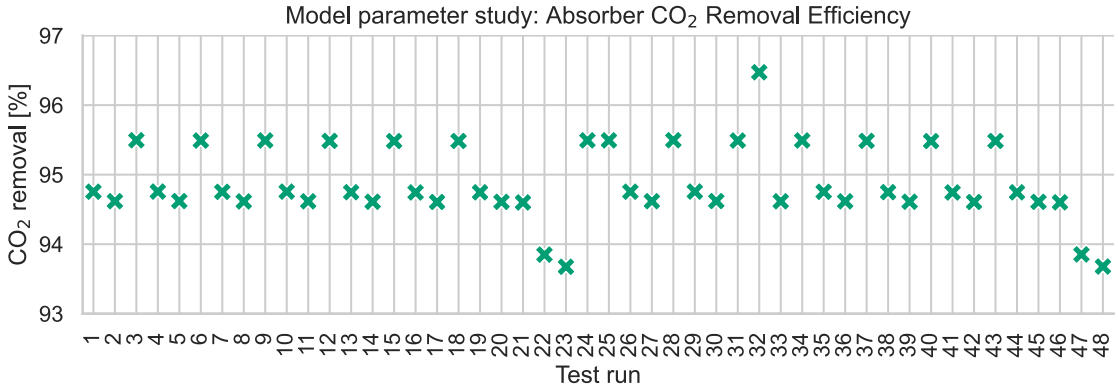

Figure 4.16: Results from the model parameter study where CO_2 removal over the absorber is plotted against the test runs.

In figure 4.17, 4.18, and 4.19, all combinations predict very similar performance except the combinations which utilise the Chen-Chuang model in the regenerator.

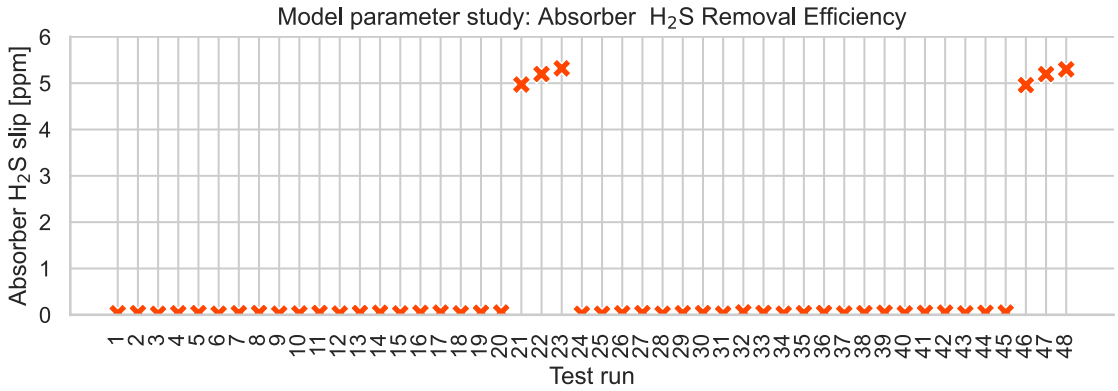

Figure 4.17: Results from the model parameter study where H_2S slip after the absorber is plotted against the test runs.

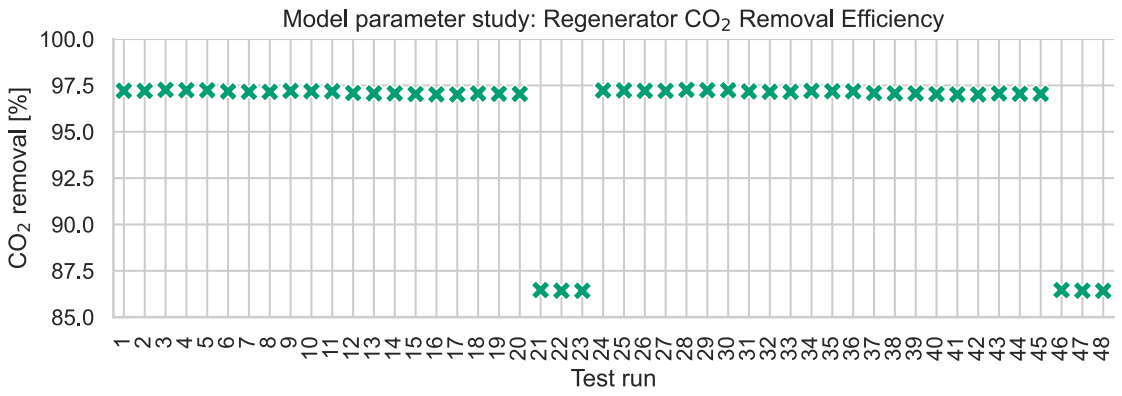

Figure 4.18: Results from the model parameter study where CO_2 removal over the regenerator is plotted against the test runs.

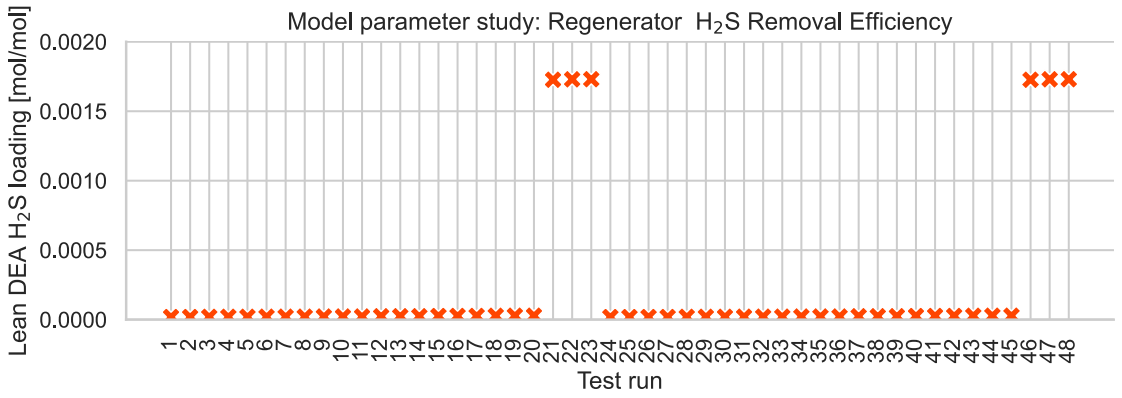

Figure 4.19: Results from the model parameter study where lean DEA H_2S loading after the regenerator is plotted against the test runs. Note that the unit is in mol/mol.

In conclusion, it is clear that different tray and mass transfer models play a small role in these specific models and that good experimental and clean DCS data are of higher importance.

5

Discussion

5.1 Can selectivity be improved by changing operating conditions?

Reboiler duty for the GPU regenerator impacts how loaded the lean amine is, but does not affect the absorber performance. Models indicate that higher reboiler duty would increase CO_2 removal and decrease H_2S slip. For CO_2, this is probably due to the absorber not being either lean amine or rich amine pinched, but somewhere in the middle, just being limited by kinetics. H_2S is possibly lean amine pinched, since the absorber slip is very low. For the TGTU, the selectivity can be heavily improved by adjusting the lean amine temperature, which almost immediately decreases CO_2 absorption by limiting the kinetically limited CO_2 absorption. H_2S slip did decrease with lower lean MDEA temperatures, and this could be explained by higher equilibrium solubility.

When changing the amine flow rate, the model seems to predict that it is possible to alter the amines' selectivity to a small extent. The sensitivity analysis on amine flow rate concludes that H_2S slip is kept low during a larger span of flow rates, compared to the CO_2 removal, which varies more. It is however, unclear how this would have worked on the real GPU amine unit, since this flow rate was not varied in the experimental runs.

Modelling results indicate that higher concentrations should slightly increase CO_2 absorption and decrease H_2S slip. The results from the GPU test runs lack low concentration results, and no conclusion could be drawn. No experimental conclusions could be drawn on amine concentration due to a large experimental spread and few test runs at low concentration.

5.2 How much can the results from experimental runs and modelling of the GPU plant transfer to the TGTU absorber and potentially increase its selectivity towards hydrogen sulfide?

Not much, the units behave differently. The TGTU absorber seems to be lean amine pinched due to its heavy decrease in H_2S slip when decreasing the tem-

perature. The GPU absorber is neither lean amine nor rich amine pinched and behaves differently.

5.3 Impact of regenerator reboiler duty on absorber performance

The results indicate that the regenerator reboiler duty has little to no impact on GPU absorber performance, regardless of the unit's operating mode. In Table 5.1, absorber performance is compared between Runs 2 and 3, and Runs 4 and 5. It is evident that reducing the reboiler duty does not lead to any detectable decline in performance.

Table 5.1: Direct comparison between steam to reboiler/lean amine flow ratio and absorber performance between comparable runs.

Comparison	Mode	Steam to reboiler/lean amine flow ratio	CO_2 removal	H_2S slip
Run 2	CFA	0,140	-88.8%	4 ppm
Run 3	CFA	0,109	-92.3%	1 ppm
Change:		**-23.3%**	**+3.9%**	**+75%**
Run 4	UCO	0,142	-85.5%	1 ppm
Run 5	UCO	0,109	-90.0%	1 ppm
Change:		**-23.0%**	**+5.3%**	**0%**

This could be due to the process not being either rich or lean amine pinched. Since the lean amine loading does not seem to alter the performance of the absorber to a measurable extent, this could indicate that the rich amine is not fully loaded with CO_2 when leaving the absorber. Therefore, to optimise the process, one would lower the regenerator reboiler duty until sufficient absorber performance is achieved. This could not be done in this thesis, since the reflux water flow in the regenerator became so low that it risked damaging the reflux pump. Therefore, it would be recommended to install a recirculation line from the pump's pressure side back to the suction side to limit problems when the unit may benefit from a lower reboiler duty or to keep operating at roughly 0,122 of steam flow/lean amine flow ratio, since this yields a minimum amount of reflux water.

5.4 Which combination of operating parameters should be run on the amine units?

All experimental runs achieved the communicated goal of 99% removal of H_2S and roughly 90% removal of CO_2. Therefore, the lower reboiler duty is to be rec-

ommended, since the amine unit still achieves its goal. For amine concentration, the result is not conclusive, and more testing is needed. Following the experimental runs conducted as part of this thesis, St1 Refinery has reduced the reboiler duty to the minimum level that does not damage the reflux pumps.

By analysing the test run results from the TGTU, a higher lean amine temperature is the easiest way to increase CO_2 absorption, and the theory agrees with this, since CO_2 absorption is kinetically limited. St1 Refinery has, after the experimental runs conducted as part of this thesis, lowered the TGTU lean amine temperature.

5.5 Liquid carry-over in amine regenerators

Regenerator reflux water had a consistently high amine concentration in all the test runs, both for the TGTU and the GPU amine unit. Due to the amines' relatively high boiling point, no amine or very small concentrations of amine should realistically be present in the condenser, and therefore, it is relevant to accept that entrainment is the cause of this. Compared to other case studies conducted by Lieberman and Ashis, both of St1 Refinery's amine unit regenerators work reasonably well at their assigned tasks, compared to the discussed regenerators in the case studies where they have large problems [40, 41].

Both the GPU and TGTU regenerators are designed with wash trays over the rich amine inlet to stop liquid entrainment, but this thesis concludes that these are not sufficient to stop carry-over.

Since both units operate full reflux condensers, loss of amine is mostly a non-problem. However, there are situations where bleeding of reflux water is recommended, such as when high amounts of corrosive contaminants like ammonium are detected by routine sampling. This thesis has observed a problem with St1 Refinery's analysis method for ammonium, which is further discussed in Section 5.6.

5.6 Problems with analysis method for ammonium in reflux water

The method for analysis of ammonium in reflux waters is based on standard ISO 7150, where St1 Refinery utilises instruments from Hach-Lange, which are known to be cross-sensitive to primary amines, mentioned in the method data sheet [45]. As seen in Figure 5.1, where the amine concentrations from the test runs are plotted against the ammonium (NH_4+) concentrations, the results correlate well with each other. This means that the method is potentially sensitive to secondary amines as well. Additionally, the method may be sensitive to tertiary amines, however more data points are required to support this.

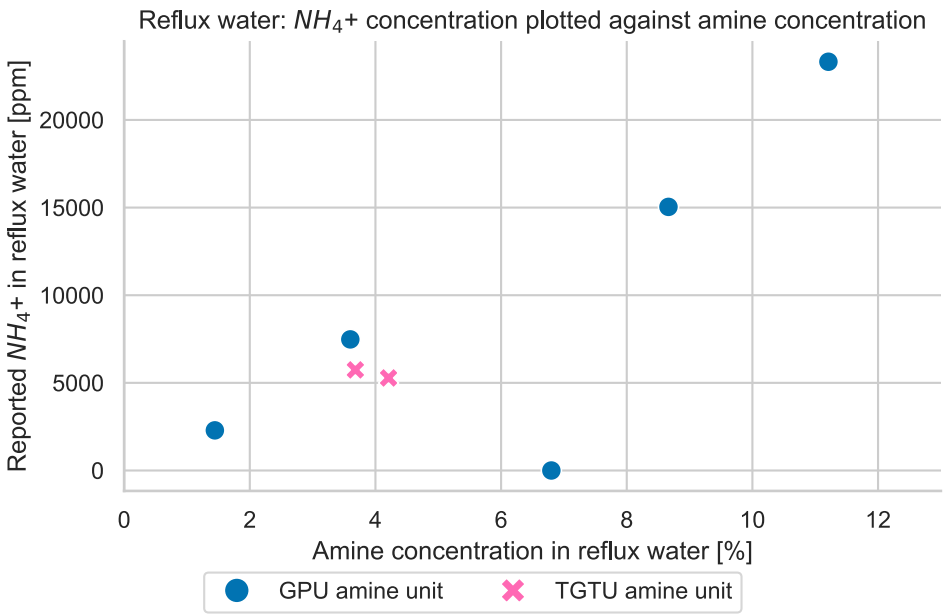

Figure 5.1: Amine concentration in reflux water plotted against reported ammonium concentration.

Therefore, the ammonium concentration results are considered invalid and not further discussed in this thesis.

5.7 Sensitivity analysis of gas flow meters and excessive flashing in rich amine drum

Orifice-based flow meters have an inherent problem that when gas density changes, they may under- or overreport flows. Therefore, for this thesis, the gas flows have been corrected for the sampled density. They are then further verified against a mass balance iterated using the regenerator CO_2 balance and the experimental GC results from the absorber gas inlet and outlet. If these calculated values are plotted against the density corrected flow meters, seen in Figure 5.2, it is clear that test runs 2 to 4 have good correspondence and that test run 1 is the only test run to have a deviation larger than 15%.

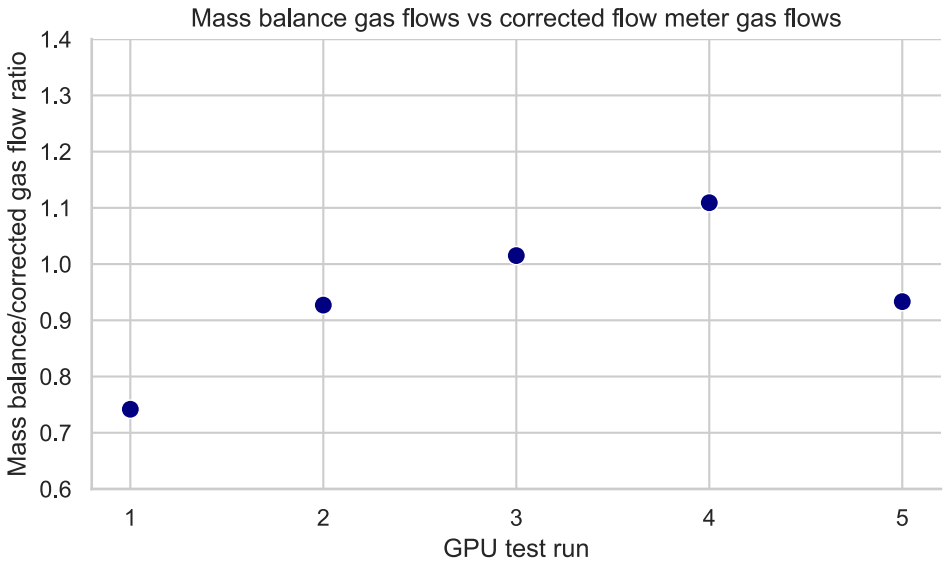

Figure 5.2: Calculated flows from mass balance compared to corrected measured flows from the DCS. Note that the mass balance flow for test run 5 is based on the Dräger analysis, since the GC analysis was unpredictable. 1 is perfect, where the mass balance and corrected gas flows are equal.

This could be coupled to the unknown flow out of the flare gas absorber. This thesis assumes that all flashing CO_2 and H_2S in the rich amine drum is reabsorbed into the DEA solution in the flare gas absorber. As an indicator of how much gases exit the flare gas absorber, one could follow how much the pressure control valve, which is fitted downstream the drum, is open. It is an unlinear control valve which, according to its design specification with 0,3 bar(g) in backpressure, lets around 10 kg/h of flash gases through at 19% opening and around 100 kg/h at 80% opening. At GPU test run 1 to 3, the valve were open between 8 and 12% which corresponds to a very small flow, which would neglibly affect the mass balance. However, at run 4 and 5, the valve were open between 59% and 64%, which would correspond to larger flows, but the amount of H_2S and CO_2 before the absorber would be very small, and after the absorber close to negligible. This could however result in a small mass balance error on these runs.

5.8 Modelling the regenerator by steam to the reboiler flow rate or the reflux flow rate

In this thesis, to calculate the reboiler duty, the flow of steam to the reboiler was gathered from a flow meter. Likewise, the reflux water flow was gathered from a flow meter. Reboiler duty affects how much water is evaporated in the regenerator and therefore is very linear with the reflux water flow, as can be seen for the GPU test runs in Figure 5.3, where it is clear that if trusting the steam flow rate leads to higher reflux mass flows than trusting the reflux flow rate. Both flow meters could ultimately diverge from the real flows.

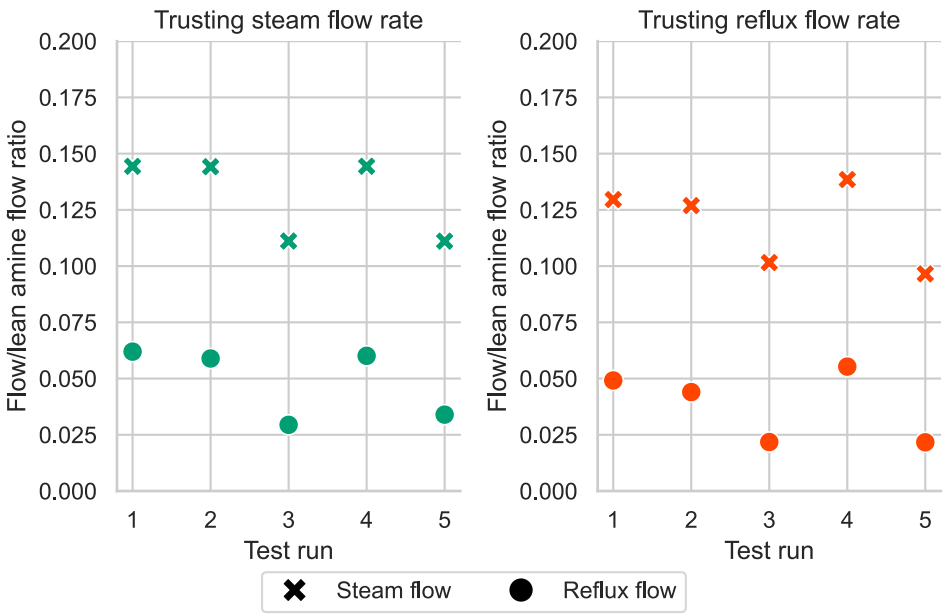

Figure 5.3: Plot where on the left-hand side the regenerator solo models for the GPU test runs are specified by the steam flow rate, and the resulting reflux flow ratio is plotted on the same axis. On the right-hand side, the same procedure is done after trusting the reflux flow rate.

In HYSYS, one can specify a column by either the reboiler duty or the reflux mass flow. If specifying the reflux mass flow, HYSYS calculates the reboiler duty, and vice versa. In Figure 5.4, the GPU solo regenerator models have been running either specified by the reflux flow meter or by the steam flow meter. Since trusting the reflux flow meter results in lower steam flows, the model predicts closer to the experimental results, since the regenerator was overpredicting for all runs. Noteworthy is that the solo models do not have the entrainment model; therefore, in the reflux flows gathered from the DCS system, there may be part resulting from entrainment instead of boil-up. Directionally, if entrainment is happening, as indicated by the reflux DEA concentration, the measured reflux flows contain water and entrainment, which would lower the steam flow further. This would ultimately have led to the models predicting closer to the experimental results.

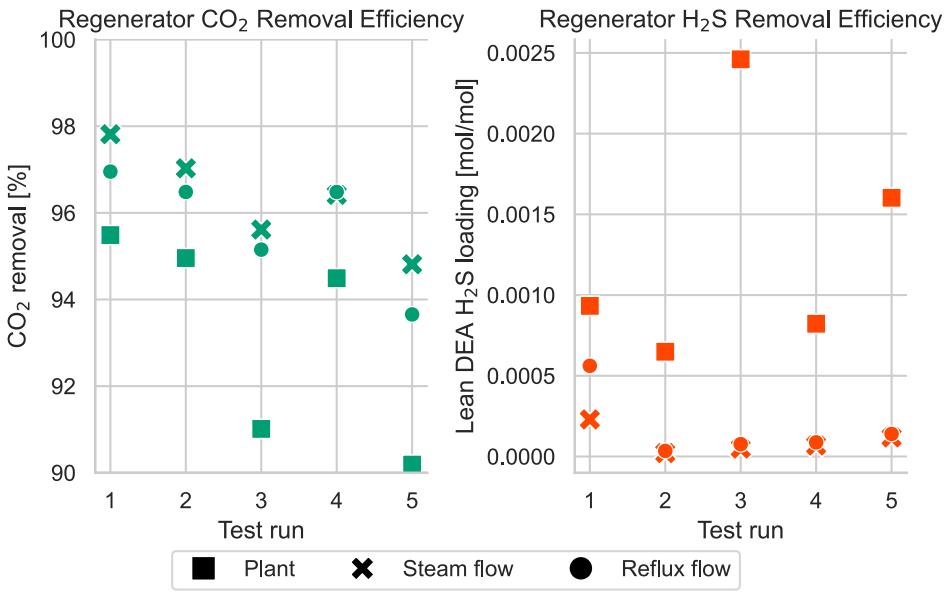

Figure 5.4: Plot where the regenerator performance for both CO_2 and H_2S is plotted after either trusting the steam flow meter or the reflux flow meter. The model results can then be compared against the experimental results.

5.9 Can the same model predict different operating scenarios?

Yes, the models seem to capture the differences between runs, but better, they act as a helpful way of predicting problems with the units by comparing an ideal case with a real scenario. The models can help identify what is not working sufficiently and what is a bad actor. For example, in the TGTU regenerator, the models predict much better performance than the unit is doing; this could, for example, be due to the formation of degradation products and/or heat-stable salts (HSS). The unit had at the time of testing been running for approximately 2 years without changing its amine solution. SRUs sometimes suffer from SO_2 slip, which heavily degrades the amine [9]. By continuously following up on the performance of the unit and comparing it with a process model, an engineer working with the unit can help to spot problems before the unit malfunctions.

6

Conclusions

This thesis has explored the selective and non-selective absorption of hydrogen sulphide (H_2S) and carbon dioxide (CO_2) in amine treating units, focusing on the modelling and optimisation of these units within a complex refinery setting. This study aimed to identify optimal operating parameters for a GPU and a TGTU and potentially find ways to improve DEA and MDEA selectivity in amine treating units. Key findings include:

- It is possible to improve selectivity by changing common operating parameters. However, to what extent is not easily determined. The lean amine temperature is the most conclusive way of increasing selectivity.
- Rate-based modelling can help to identify bad actors in amine treating systems and explore alternative operating parameters.
- Reboiler duty for the GPU amine unit should be kept low, since in this case, when the absorber is neither lean nor rich amine pinched, it does have very little impact on the absorber performance.
- Optimum amine flow rate should be determined after finding the lowest reboiler duty that the GPU unit can run stably.
- For the TGTU, lean amine temperature should be kept low to decrease CO_2 absorption. This reduces the accumulation of CO_2 in the SRU and slip of H_2S to downstream units.

7

References

[1] Marc J Ledoux et al. “Selective oxidation of H2S in Claus tail-gas over SiC supported NiS2 catalyst”. In: *Catalysis Today* 61.1–4 (Aug. 2000), pp. 157–163. ISSN: 0920-5861. DOI: 10.1016/s0920-5861(00)00365-5. URL: http://dx.doi.org/10.1016/S0920-5861(00)00365-5.

[2] Jadwiga Więckowska. “Catalytic and adsorptive desulphurization of gases”. In: *Catalysis Today* 24.4 (July 1995), pp. 405–465. ISSN: 0920-5861. DOI: 10.1016/0920-5861(95)00021-7. URL: http://dx.doi.org/10.1016/0920-5861(95)00021-7.

[3] Stefania Gardarsdottir et al. “Preem CCS – A Pioneering Swedish-Norwegian Collaboration Showcasing the Full CCS Chain”. In: *SSRN Electronic Journal* (2021). ISSN: 1556-5068. DOI: 10.2139/ssrn.3820698. URL: http://dx.doi.org/10.2139/ssrn.3820698.

[4] Daniel Garraín et al. “Renewable Diesel Fuel from Processing of Vegetable Oil in Hydrotreatment Units: Theoretical Compliance with European Directive 2009/28/EC and Ongoing Projects in Spain”. In: *Smart Grid and Renewable Energy* 01 (Jan. 2010), pp. 70–73. DOI: 10.4236/sgre.2010.12011.

[5] Hannu Aatola et al. “Hydrotreated Vegetable Oil (HVO) as a Renewable Diesel Fuel: Trade-off between NOx, Particulate Emission, and Fuel Consumption of a Heavy Duty Engine”. In: *SAE International Journal of Engines* 1.1 (Oct. 2008), pp. 1251–1262. ISSN: 1946-3944. DOI: 10.4271/2008-01-2500. URL: http://dx.doi.org/10.4271/2008-01-2500.

[6] Bambang Veriansyah et al. “Production of renewable diesel by hydroprocessing of soybean oil: Effect of catalysts”. In: *Fuel* 94 (Apr. 2012), pp. 578–585. ISSN: 0016-2361. DOI: 10.1016/j.fuel.2011.10.057. URL: http://dx.doi.org/10.1016/j.fuel.2011.10.057.

[7] Stéphanie Bouckaert et al. *Net Zero by 2050: A Roadmap for the Global Energy Sector*. Tech. rep. International Energy Agency, Oct. 2021. URL: https://www.iea.org/reports/net-zero-by-2050.

[8] Bishnupada Mandal and Shyamalendu S. Bandyopadhyay. “Simultaneous Absorption of CO2 and H2S Into Aqueous Blends of N-Methyldiethanolamine and Diethanolamine”. In: *Environmental Science & Technology* 40.19 (2006), pp. 6076–6084. DOI: 10.1021/es0606475. eprint: https://doi.org/10.1021/es0606475. URL: https://doi.org/10.1021/es0606475.

[9] Arthur L. Kohl and Richard Nielsen. “Gas Purification”. In: 5th. Elsevier Science & Technology, Aug. 1997. Chap. 1. Introduction, p. 39. ISBN: 9780080507200.

[10] R. R. Bottoms. “Organic Bases for Gas Purification”. In: *Industrial & Engineering Chemistry* 23.5 (May 1931), pp. 501–504. ISSN: 1541-5724. DOI: 10.1021/ie50257a007. URL: http://dx.doi.org/10.1021/ie50257a007.

[11] H. D. Frazier and A. L. Kohl. “Selective Absorption of Hydrogen Sulfide from Gas Streams”. In: *Industrial & Engineering Chemistry* 42.11 (Nov. 1950), pp. 2288–2292. ISSN: 1541-5724. DOI: 10.1021/ie50491a032. URL: http://dx.doi.org/10.1021/ie50491a032.

[12] Ashis Nag. “6. Amine Regeneration Units”. In: *Distillation & Hydrocarbon Processing Practices*. PennWell, 2016. ISBN: 978-1-59370-343-1. URL: https://app.knovel.com/hotlink/khtml/id:kt0113KOI1/distillation-hydrocarbon/amine-carryover-reflux.

[13] Raymond A. Tomcej and Fred D. Otto. “Absorption of CO2 and N2O into aqueous solutions of methyldiethanolamine”. In: *AIChE Journal* 35.5 (May 1989), pp. 861–864. ISSN: 1547-5905. DOI: 10.1002/aic.690350519. URL: http://dx.doi.org/10.1002/aic.690350519.

[14] Karen Gonzalez et al. “CO2 and H2S absorption in aqueous MDEA with ethylene glycol: Electrolyte NRTL, rate-based process model and pilot plant experimental validation”. In: *Chemical Engineering Journal* 451 (Jan. 2023), p. 138948. ISSN: 1385-8947. DOI: 10.1016/j.cej.2022.138948. URL: http://dx.doi.org/10.1016/j.cej.2022.138948.

[15] B.P Mandal, A.K Biswas, and S.S Bandyopadhyay. “Selective absorption of H2S from gas streams containing H2S and CO2 into aqueous solutions of N-methyldiethanolamine and 2-amino-2-methyl-1-propanol”. In: *Separation and Purification Technology* 35.3 (Mar. 2004), pp. 191–202. ISSN: 1383-5866. DOI: 10.1016/s1383-5866(03)00139-4. URL: http://dx.doi.org/10.1016/S1383-5866(03)00139-4.

[16] Michael Caplow. “Kinetics of carbamate formation and breakdown”. In: *Journal of the American Chemical Society* 90.24 (Nov. 1968), pp. 6795–6803. ISSN: 1520-5126. DOI: 10.1021/ja01026a041. URL: http://dx.doi.org/10.1021/ja01026a041.

[17] Terrence L. Donaldson and Yen N. Nguyen. “Carbon Dioxide Reaction Kinetics and Transport in Aqueous Amine Membranes”. In: *Industrial & Engineering Chemistry Fundamentals* 19.3 (Aug. 1980), pp. 260–266. ISSN: 1541-4833. DOI: 10.1021/i160075a005. URL: http://dx.doi.org/10.1021/i160075a005.

[18] D. W. Savage and C. J. Kim. “Chemical kinetics of carbon dioxide reactions with diethanolamine and diisopropanolamine in aqueous solutions”. In: *AIChE Journal* 31.2 (Feb. 1985), pp. 296–301. ISSN: 1547-5905. DOI: 10.1002/aic.690310217. URL: http://dx.doi.org/10.1002/aic.690310217.

[19] H. Hikita et al. “The kinetics of reactions of carbon dioxide with monoethanolamine, diethanolamine and triethanolamine by a rapid mixing method”. In: *The Chemical Engineering Journal* 13.1 (1977), pp. 7–12.

ISSN: 0300-9467. DOI: 10.1016/0300-9467(77)80002-6. URL: http://dx.doi.org/10.1016/0300-9467(77)80002-6.

[20] S.S. Laddha and P.V. Danckwerts. “Reaction of CO2 with ethanolamines: kinetics from gas-absorption”. In: *Chemical Engineering Science* 36.3 (1981), pp. 479–482. ISSN: 0009-2509. DOI: 10.1016/0009-2509(81)80135-2. URL: http://dx.doi.org/10.1016/0009-2509(81)80135-2.

[21] Ridha Ben Said et al. “A Unified Approach to CO2–Amine Reaction Mechanisms”. In: *ACS Omega* 5.40 (Oct. 2020), pp. 26125–26133. ISSN: 2470-1343. DOI: 10.1021/acsomega.0c03727. URL: http://dx.doi.org/10.1021/acsomega.0c03727.

[22] B.P. Mandal and S.S. Bandyopadhyay. “Simultaneous absorption of carbon dioxide and hydrogen sulfide into aqueous blends of 2-amino-2-methyl-1-propanol and diethanolamine”. In: *Chemical Engineering Science* 60.22 (Nov. 2005), pp. 6438–6451. ISSN: 0009-2509. DOI: 10.1016/j.ces.2005.02.044. URL: http://dx.doi.org/10.1016/j.ces.2005.02.044.

[23] Hamid Reza Godini and Dariush Mowla. “Selectivity study of H2S and CO2 absorption from gaseous mixtures by MEA in packed beds”. In: *Chemical Engineering Research and Design* 86.4 (Apr. 2008), pp. 401–409. ISSN: 0263-8762. DOI: 10.1016/j.cherd.2007.11.012. URL: http://dx.doi.org/10.1016/j.cherd.2007.11.012.

[24] David W. Savage et al. “Selective absorption of hydrogen sulfide and carbon dioxide into aqueous solutions of methyldiethanolamine”. In: *Industrial & Engineering Chemistry Fundamentals* 25.3 (Aug. 1986), pp. 326–330. ISSN: 1541-4833. DOI: 10.1021/i100023a004. URL: http://dx.doi.org/10.1021/i100023a004.

[25] Gianni Astarita and David W. Savage. “Gas absorption and desorption with reversible instantaneous chemical reaction”. In: *Chemical Engineering Science* 35.8 (1980), pp. 1755–1764. ISSN: 0009-2509. DOI: 10.1016/0009-2509(80)85011-1. URL: http://dx.doi.org/10.1016/0009-2509(80)85011-1.

[26] R.J. Littel et al. “Modelling of simultaneous absorption of H2S and CO2 in alkanolamine solutions: The influence of parallel and consecutive reversible reactions and the coupled diffusion of ionic species”. In: *Chemical Engineering Science* 46.9 (1991), pp. 2303–2313. ISSN: 0009-2509. DOI: 10.1016/0009-2509(91)85128-k. URL: http://dx.doi.org/10.1016/0009-2509(91)85128-K.

[27] J. David Lawson and A. W. Garst. “Gas sweetening data: equilibrium solubility of hydrogen sulfide and carbon dioxide in aqueous monoethanolamine and aqueous diethanolamine solutions”. In: *Journal of Chemical & Engineering Data* 21.1 (1976), pp. 20–30. DOI: 10.1021/je60068a010. URL: https://doi.org/10.1021/je60068a010.

[28] AspenTech. *Acid Gas Cleaning Using Amine Solvents: Validation with Experimental and Plant Data*. White paper. 2019.

[29] Ying Zhang and Chau-Chyun Chen. “Thermodynamic Modeling for CO2 Absorption in Aqueous MDEA Solution with Electrolyte NRTL Model”. In: *Industrial & Engineering Chemistry Research* 50.1 (Aug. 2010), pp. 163–

175. ISSN: 1520-5045. DOI: 10.1021/ie1006855. URL: http://dx.doi.org/10.1021/ie1006855.

[30] Wei-Chung Yu and Gianni Astarita. “Selective absorption of hydrogen sulphide in tertiary amine solutions”. In: *Chemical Engineering Science* 42.3 (1987), pp. 419–424. ISSN: 0009-2509. DOI: 10.1016/0009-2509(87)80004-0. URL: http://dx.doi.org/10.1016/0009-2509(87)80004-0.

[31] Yu. A. Anufrikov, G. L. Kuranov, and N. A. Smirnova. “Solubility of CO_2 and H2S in alkanolamine-containing aqueous solutions”. In: *Russian Journal of Applied Chemistry* 80.4 (Apr. 2007), pp. 515–527. ISSN: 1608-3296. DOI: 10.1134/s1070427207040015. URL: http://dx.doi.org/10.1134/S1070427207040015.

[32] P.J.G. Huttenhuis et al. “Gas solubility of H2S and CO2 in aqueous solutions of N-methyldiethanolamine”. In: *Journal of Petroleum Science and Engineering* 55.1–2 (Jan. 2007), pp. 122–134. ISSN: 0920-4105. DOI: 10.1016/j.petrol.2006.04.018. URL: http://dx.doi.org/10.1016/j.petrol.2006.04.018.

[33] Laura A. Pellegrini et al. “Design of an acidic natural gas purification plant by means of a process simulator”. In: *Chemical Engineering Transactions* 24 (Apr. 2011), pp. 271–276. DOI: 10.3303/CET1124046. URL: https://doi.org/10.3303/CET1124046.

[34] S. Moioli, L.A. Pellegrini, and S. Gamba. “Simulation of CO2 Capture by MEA Scrubbing with a Rate-Based Model”. In: *Procedia Engineering* 42 (2012), pp. 1651–1661. ISSN: 1877-7058. DOI: 10.1016/j.proeng.2012.07.558. URL: http://dx.doi.org/10.1016/j.proeng.2012.07.558.

[35] R. Kuroda, P. Chandran, and R. Weiland. “Amine strength in gas treatment”. In: *Hydrocarbon Processing* (June 2024). URL: https://www.hydrocarbonprocessing.com/magazine/2024/june-2024/special-focus-process-optimization/amine-strength-in-gas-treatment/.

[36] Jian-Gang Lu, You-Fei Zheng, and Du-Liang He. “Selective absorption of H2S from gas mixtures into aqueous solutions of blended amines of methyldiethanolamine and 2-tertiarybutylamino-2-ethoxyethanol in a packed column”. In: *Separation and Purification Technology* 52.2 (Dec. 2006), pp. 209–217. ISSN: 1383-5866. DOI: 10.1016/j.seppur.2006.04.003. URL: http://dx.doi.org/10.1016/j.seppur.2006.04.003.

[37] Idris Mohamed Saeed et al. “Thermal degradation of diethanolamine at stripper condition for CO2 capture: Product types and reaction mechanisms”. en. In: *Chin. J. Chem. Eng.* 27.12 (Dec. 2019), pp. 2900–2908.

[38] C. J. Kim and G. Sartori. “Kinetics and mechanism of diethanolamine degradation in aqueous solutions containing carbon dioxide”. In: *International Journal of Chemical Kinetics* 16.10 (Oct. 1984), pp. 1257–1266. ISSN: 1097-4601. DOI: 10.1002/kin.550161008. URL: http://dx.doi.org/10.1002/kin.550161008.

[39] Walaa Shehata et al. “Challenges and Solutions of Gas Sweetening Unit in Polypropylene Plant using Process Simulation: A Case Study”. In: *Petroleum and Coal* 61 (May 2019), pp. 517–532. ISSN: 1337-7027.

[40] Norman P. Lieberman. “19.2 Amine Regenerator”. In: *Troubleshooting Process Operations*. 5th. PennWell, 2024. ISBN: 978-1-955578-20-2. URL: https://app.knovel.com/hotlink/khtml/id:kt0141R7R2/troubleshooting-process/amine-regenerator.

[41] Ashis Nag. “6.8.3.1 Amine Carryover to the Reflux Drum”. In: *Distillation & Hydrocarbon Processing Practices*. PennWell, 2016. ISBN: 978-1-59370-343-1. URL: https://app.knovel.com/hotlink/khtml/id:kt0113KOI1/distillation-hydrocarbon/amine-carryover-reflux.

[42] Ying Zhang et al. “Rate-Based Process Modeling Study of CO2 Capture with Aqueous Monoethanolamine Solution”. In: *Industrial & Engineering Chemistry Research* 48.20 (Sept. 2009), pp. 9233–9246. ISSN: 1520-5045. DOI: 10.1021/ie900068k. URL: http://dx.doi.org/10.1021/ie900068k.

[43] Swedegas. *Gaskvaliteten följs noggrant*. Mar. 2025. URL: https://swedegas.se/gas/gaskvalitet.

[44] Michael Sheilan and Benjamin Spooner. “The Seven Deadly Sins of Amine Treating of Natural Gas Streams”. In: *Amine Treating & Sour Water Stripping*. 13th. Sulphur Experts, 2022.

[45] Hach Lange GmbH. *Sulfide, Methylene Blue Method (800 μg/L)*. Ed. 11. Sept. 2018. URL: https://images.hach.com/asset-get.download.jsa?id=7639983902.

A

Calculations

A.1 Nomenclature

- ρ_{tot} - Density of total sample (kg/m^3)
- γ_i - Mass concentration of species i (g/l)
- Y_i - Mass fraction of species i
- M_i = Molar mass of species i(g/mol)
- Q_{DCS} = Flow meter reading from digital control system (T/D)
- Q_{corr} = Corrected flow meter reading

A.2 DEA loading (mol(gas)/mol(amine)) from concentration

Sour gas loadings from the laboratory are reported in grams of sour gas per litre of amine solution. To get the established measurement of amine loading, mol_{gas}/mol_{amine}, the following calculations are performed.

A.2.1 Amine mole count

Mass concentrations, density of total sample and DEA-concentration were gathered from laboratory results for the lean DEA sample. In Equation A.1, the total mole count per kg of sample is calculated by multiplying by the DEA fraction of the sample.

$$\frac{mol_{amine}}{kg} = \frac{(\rho_{tot} - \gamma_{CO_2} - \gamma_S) * Y_{lean\ amine}}{M_{amine}} \tag{A.1}$$

If the amine is assumed to degrade negligibly and no amine is assumed to be lost over head, the total mole count of the lean and rich amine can be assumed to be the same. The ratio between water and amine is assumed to be the same. The

ratio is calculated according to Equation A.2

$$\frac{\text{kg amine}}{\text{m}^3} = (\rho_{\text{tot}} - \gamma_{CO_2} - \gamma_S) * Y_{\text{lean amine}} \tag{A.2a}$$

$$\frac{\text{kg } H_2O}{\text{m}^3} = (\rho_{\text{tot}} - \gamma_{CO_2} - \gamma_S) - \frac{\text{kg amine}}{\text{m}^3} \tag{A.2b}$$

$$H_2O\text{/amine ratio} = \frac{\frac{\text{kg amine}}{\text{m}^3}}{\frac{\text{kg } H_2O}{\text{m}^3}} \tag{A.2c}$$

This ratio is used in Equation A.3 to calculate the rich amine concentration, which then can be used in the same way as for Equation A.1 to calculate the amine molar count.

$$\frac{\text{kg } H_2O \text{ and amine in rich sample}}{\text{m}^3} = (\rho_{\text{tot}} - \gamma_{CO_2} - \gamma_S) \tag{A.3a}$$

$$\frac{\text{kg amine in rich sample}}{\text{m}^3} = \frac{\text{kg } H_2O \text{ and amine in rich sample}}{\text{m}^3} * H_2O\text{/amine ratio} \tag{A.3b}$$

$$\frac{\text{kg } H_2O \text{ in rich sample}}{\text{m}^3} = \frac{\text{kg } H_2O \text{ and amine in rich sample}}{\text{m}^3} - \frac{\text{kg amine in rich sample}}{\text{m}^3} \tag{A.3c}$$

$$Y_{\text{rich amine}} = \frac{\frac{\text{kg amine in rich sample}}{\text{m}^3}}{\frac{\text{kg } H_2O \text{ in rich sample}}{\text{m}^3} + \frac{\text{kg amine in rich sample}}{\text{m}^3} + \gamma_{CO_2} + \gamma_S} \tag{A.3d}$$

A.2.2 Rich and lean amine sour gas loading

To calculate sour gas loadings, the measured mass concentration of either CO_2 or S was gathered and converted to moles per kg. Then these values were divided by the values from Equation A.1 to get the correct unit of amine loading, $\text{mol}_{\text{gas}}/\text{mol}_{\text{amine}}$.

For CO_2 the calculations can be seen in Equation A.4:

$$\frac{\text{mol}_{CO_2}}{\text{kg}} = \frac{\gamma_{CO_2}/\rho_{\text{tot}}}{M_{CO_2}} \tag{A.4a}$$

$$\frac{\text{mol}_{CO_2}}{\text{mol}_{\text{DEA}}} = \frac{\frac{\text{mol}_{CO_2}}{\text{kg}}}{\frac{\text{mol}_{\text{DEA}}}{\text{kg}}} \tag{A.4b}$$

For sulphides, the calculations can be seen in Equation A.5:

$$\frac{\text{mol}_S}{\text{kg}} = \frac{\gamma_S/\rho_{\text{tot}}}{M_S} \tag{A.5a}$$

$$\frac{mol_S}{mol_{DEA}} = \frac{\frac{mol_S}{kg}}{\frac{mol_{DEA}}{kg}} \tag{A.5b}$$

A.2.3 Assumptions

The method used to measure the total hydrogen sulphide concentration is cross-sensitive to acid-soluble metal sulphides [45]. The metal sulphide concentration is assumed to be non-existent, therefore, sulphide loading is assumed to be H_2S loading.

A.3 Corrected flows from DCS

Since gas flows from the DCS system is based around pressure differences over an orifice, they are not exact when molar weight of the gas change.

A simplified formula, seen in Equation A.6 can be used to compensate for the different molar mass of the gas, assuming incompressible flow. The gas solutions are in reality compressible, but this will significantly better the flow rate readings from DCS.

$$\frac{Q_{DCS}^2}{M_{DCS}} = \frac{Q_{corr}^2}{M_{calc}} \tag{A.6a}$$

$$Q_{corr} = Q_{DCS} * \sqrt{\frac{M_{calc}}{M_{DCS}}} \tag{A.6b}$$

Since both nitrogen and oxygen are unlikely to be in the mixture of gasses from the samples in GPU, these could be deleted, and the other components could be adjusted up. This adjusted composition could be used to calculate a corrected molar mass. The adjustment was done using HYSYS, where the molar mas was calculated as well.

IV

B

Detailed process diagrams

<

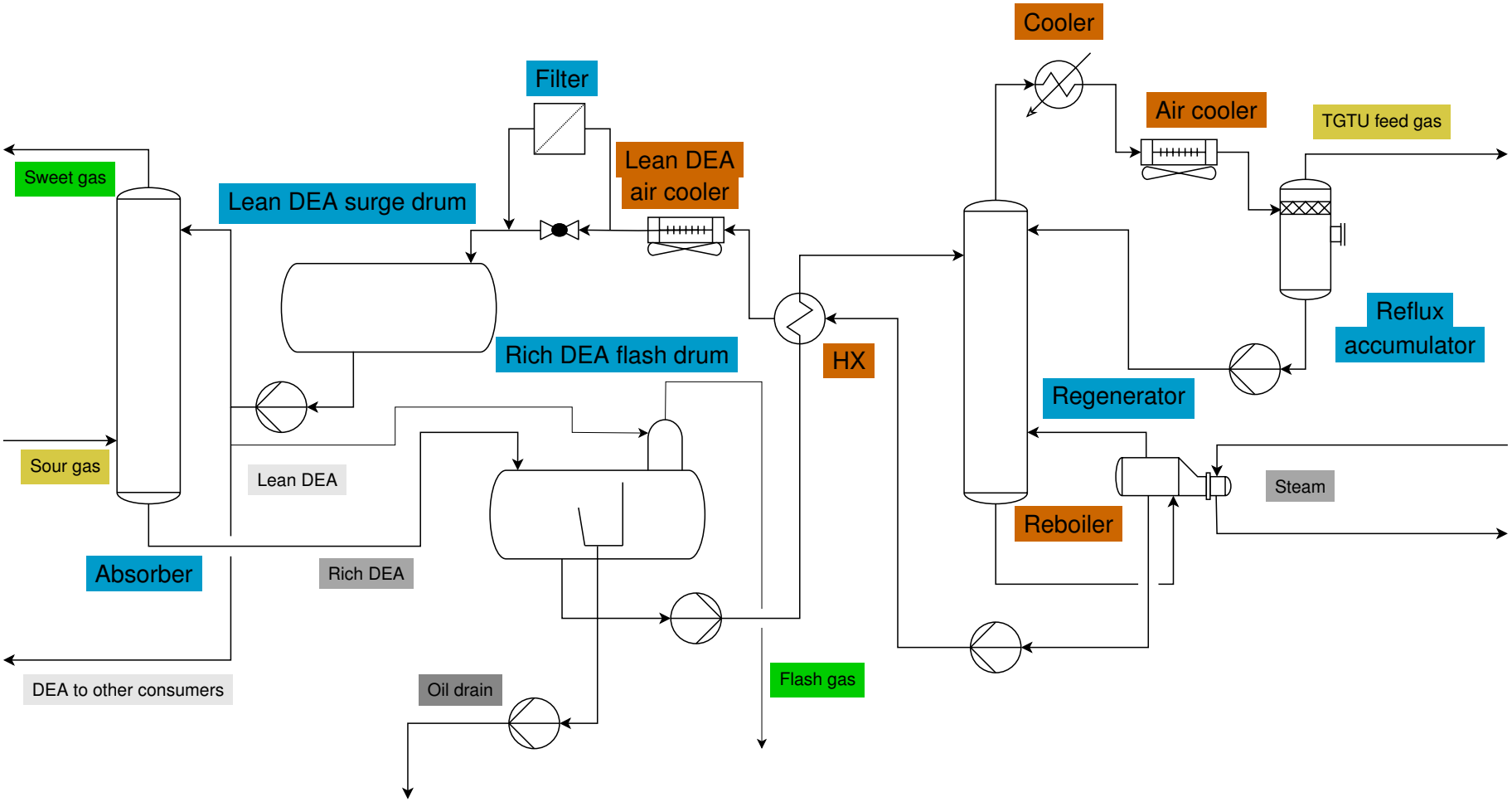

Figure B.1: St1 GPU amine treating unit process diagram. The amine unit is of a third-party design.

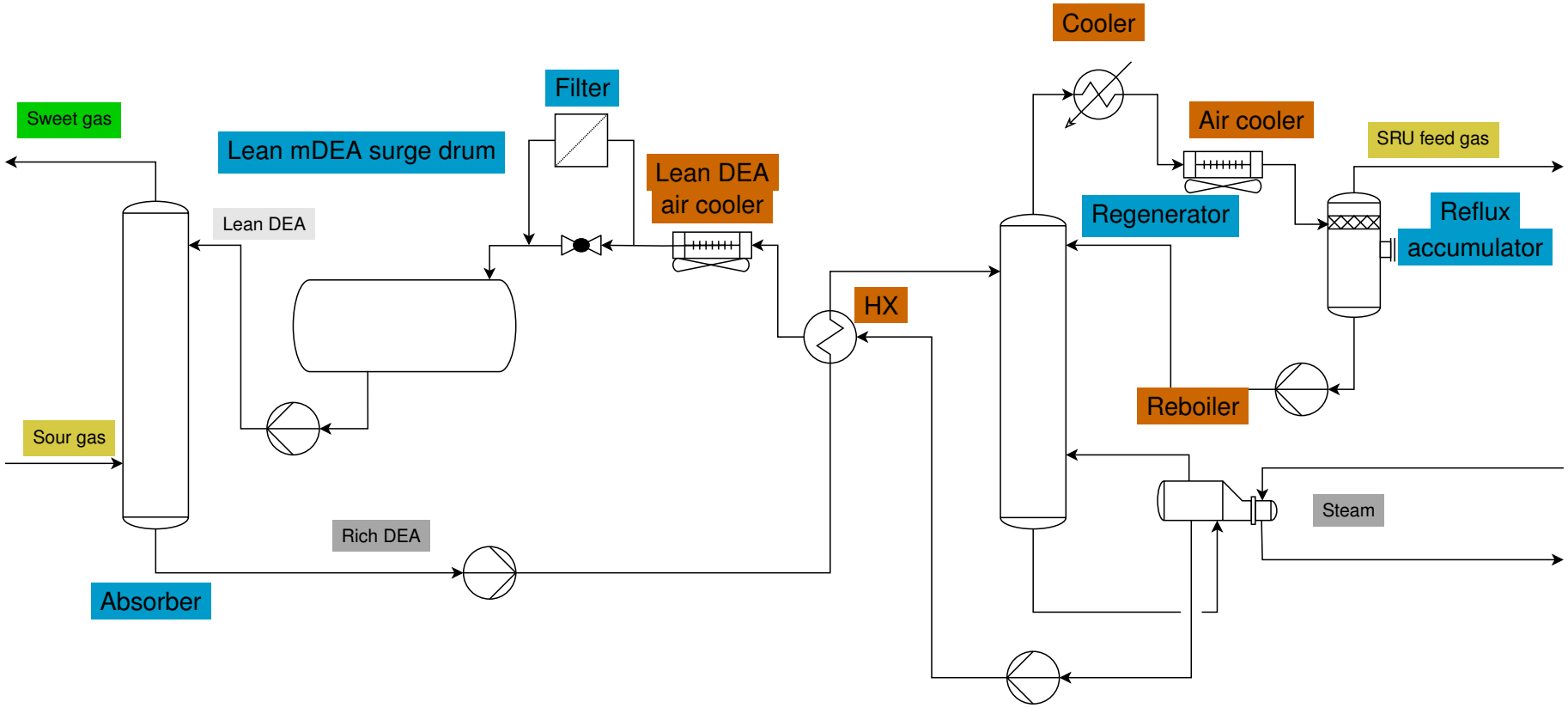

Figure B.2: St1 tail gas treating unit process diagram.

VIII

C

Column and model internals

Table C.1: Specification of models and unit internals.

Column	Diameter	Packed/trays	No. of trays/ Section packed height	Type of internals	Model internals
GPU absorber	Confidential	Confidental	Confidental	Confidential	Koch Flexitray
GPU regenerator	1100 mm	Trays	2 wash trays + 24 stripper trays	Fixed valve trays	Sieves
GPU flare gas absorber	250 mm	Packed	1000 mm	Random packing	Metal pall rings
TGTU absorber	768 mm	Packed	4578 mm	Mellapak Plus 202Y	No change
TGTU regenerator	950 mm	Mixed	2 wash trays + 8362 mm	Fixed valve trays + Mellapak 250X	Sieves as wash trays

X

D

Model parameter study

In Table D.1, which contains raw data from the model parameter study run in HYSYS, abs means absorber results, and reg means regenerator.

Table D.1: Raw data from model parameter study.

Exp	Abs. tray	Abs. model	Reg. tray	Reg. model	CO_2 lean loading	CO_2 rich loading	n (reg, CO_2) [%]	H_2S lean loading	H_2S rich loading	n (reg, H_2S) [%]	n (abs, CO_2) [%]	H_2S Sweet [ppm]
1	Koch	AIChE	Sieve	Chan-Fair	7,64E-03	0,273962	97,21	1,94E-05	1,67E-02	99,88	94,75	3,31E-02
2	Koch	Gerster	Sieve	Chan-Fair	7,64E-03	0,273579	97,21	1,94E-05	1,67E-02	99,88	94,62	3,73E-02
3	Koch	Scheffe	BDH	Scheffe	7,56E-03	0,275942	97,26	2,03E-05	1,67E-02	99,88	95,49	2,28E-02
4	Koch	AIChE	BDH	Scheffe	7,55E-03	0,273877	97,24	2,05E-05	1,67E-02	99,88	94,76	3,41E-02
5	Koch	Gerster	BDH	Scheffe	7,55E-03	0,273495	97,24	2,06E-05	1,67E-02	99,88	94,62	3,82E-02
6	Koch	Scheffe	Sieve	AIChE	7,80E-03	0,276171	97,18	2,11E-05	1,67E-02	99,87	95,49	2,43E-02
7	Koch	AIChE	Sieve	AIChE	7,79E-03	0,274106	97,16	2,13E-05	1,67E-02	99,87	94,75	3,59E-02
8	Koch	Gerster	Sieve	AIChE	7,79E-03	0,27373	97,15	2,14E-05	1,67E-02	99,87	94,61	3,97E-02

Exp	Abs. tray	Abs. model	Reg. tray	Reg. model	CO_2 lean loading	CO_2 rich loading	n (reg, CO_2) [%]	H_2S lean loading	H_2S rich loading	n (reg, H_2S) [%]	n (abs, CO_2) [%]	H_2S Sweet [ppm]
9	Koch	Scheffe	BDH	AIChE	7,72E-03	0,276093	97,21	2,22E-05	1,67E-02	99,87	95,49	2,52E-02
10	Koch	AIChE	BDH	AIChE	7,71E-03	2,74E-01	97,19	2,24E-05	1,67E-02	99,87	94,76	3,02E-02
11	Koch	Gerster	BDH	AIChE	7,71E-03	0,273645	97,18	2,25E-05	1,67E-02	99,87	94,62	4,10E-02
12	Koch	Scheffe	Sieve	Chan-Fair-RF	8,04E-03	0,276399	97,09	2,45E-05	1,67E-02	99,85	95,49	2,82E-02
13	Koch	AIChE	Sieve	Chan-Fair-RF	8,03E-03	0,274332	97,07	2,47E-05	1,67E-02	99,85	94,75	4,02E-02
14	Koch	Gerster	Sieve	Chan-Fair-RF	8,03E-03	0,273948	97,07	2,48E-05	1,67E-02	99,85	94,61	4,46E-02
15	Koch	Scheffe	Sieve	Gerster	8,20E-03	0,276548	97,04	2,67E-05	1,67E-02	99,84	95,48	3,08E-02
16	Koch	AIChE	Sieve	Gerster	8,19E-03	0,27448	97,02	2,69E-05	1,67E-02	99,84	94,74	4,32E-02
17	Koch	Gerster	Sieve	Gerster	8,19E-03	0,274096	97,01	2,70E-05	1,67E-02	99,84	94,61	4,76E-02
18	Koch	Scheffe	BDH	Gerster	8,11E-03	0,276464	97,07	2,79E-05	1,67E-02	99,83	95,48	3,19E-02
19	Koch	AIChE	BDH	Gerster	8,10E-03	0,274395	97,05	2,82E-05	1,67E-02	99,83	94,75	4,43E-02
20	Koch	Gerster	BDH	Gerster	8,10E-03	0,274012	97,04	2,83E-05	1,67E-02	99,83	94,61	4,90E-02
21	Koch	Scheffe	Sieve	Chen-Chuang	4,16E-02	0,307548	86,46	1,73E-03	1,82E-02	90,53	94,60	4,971
22	Koch	AIChE	Sieve	Chen-Chuang	4,14E-02	0,305194	86,43	1,73E-03	1,82E-02	90,51	93,85	5,198
23	Koch	Gerster	Sieve	Chen-Chuang	4,14E-02	0,304743	86,42	1,73E-03	1,82E-02	90,51	93,68	5,320
24	Koch	Scheffe	Sieve	Chan-Fair	7,65E-03	2,76E-01	97,23	1,92E-05	1,67E-02	99,88	95,49	2,21E-02
25	Nutter	Scheffe	Sieve	Chan-Fair	7,65E-03	0,276028	97,23	1,92E-05	1,67E-02	99,88	95,49	2,20E-02
26	Nutter	AIChE	Sieve	Chan-Fair	7,64E-03	0,273962	97,21	1,94E-05	1,67E-02	99,88	94,75	3,31E-02

Exp	Abs. tray	Abs. model	Reg. tray	Reg. model	CO_2 lean loading	CO_2 rich loading	n (reg, CO_2) [%]	H_2S lean loading	H_2S rich loading	n (reg, H_2S) [%]	n (abs, CO_2) [%]	H_2S Sweet [ppm]
27	Nutter	Gerster	Sieve	Chan-Fair	7,64E-03	0,27358	97,21	1,94E-05	1,67E-02	99,88	94,62	3,71E-02
28	Nutter	Scheffe	BDH	Scheffe	7,56E-03	0,275942	97,26	2,03E-05	1,67E-02	99,88	95,49	2,31E-02
29	Nutter	AIChE	BDH	Scheffe	7,55E-03	0,273877	97,24	2,05E-05	1,67E-02	99,88	94,76	3,44E-02
30	Nutter	Gerster	BDH	Scheffe	7,55E-03	0,273495	97,24	2,06E-05	1,67E-02	99,88	94,62	3,82E-02
31	Nutter	Scheffe	Sieve	AIChE	7,80E-03	0,276171	97,18	2,11E-05	1,67E-02	99,87	95,49	2,44E-02
32	Nutter	AIChE	Sieve	AIChE	7,79E-03	0,274105	97,16	2,13E-05	1,67E-02	99,87	96,47	5,33E-02
33	Nutter	Gerster	Sieve	AIChE	7,79E-03	0,273644	97,15	2,14E-05	1,67E-02	99,87	94,62	4,11E-02
34	Nutter	Scheffe	BDH	AIChE	7,72E-03	0,276093	97,21	2,22E-05	1,67E-02	99,87	95,49	2,53E-02
35	Nutter	AIChE	BDH	AIChE	7,71E-03	0,274028	97,19	2,24E-05	1,67E-02	99,87	94,75	3,67E-02
36	Nutter	Gerster	BDH	AIChE	7,71E-03	0,273644	97,18	2,25E-05	1,67E-02	99,87	94,62	4,11E-02
37	Nutter	Scheffe	Sieve	Chan-Fair-RF	8,04E-03	0,276399	97,09	2,45E-05	1,67E-02	99,85	95,49	2,82E-02
38	Nutter	AIChE	Sieve	Chan-Fair-RF	8,03E-03	0,274366	97,07	2,45E-05	1,67E-02	99,85	94,75	3,67E-02
39	Nutter	Gerster	Sieve	Chan-Fair-RF	8,03E-03	0,273948	97,07	2,48E-05	1,67E-02	99,85	94,61	4,46E-02
40	Nutter	Scheffe	Sieve	Gerster	8,20E-03	0,276548	97,04	2,67E-05	1,67E-02	99,84	95,48	3,08E-02
41	Nutter	AIChE	Sieve	Gerster	8,19E-03	0,27448	97,02	2,69E-05	1,67E-02	99,84	94,74	4,32E-02
42	Nutter	Gerster	Sieve	Gerster	8,19E-03	0,274096	97,01	2,70E-05	1,67E-02	99,84	94,61	4,76E-02
43	Nutter	Scheffe	BDH	Gerster	8,11E-03	0,276463	97,07	2,79E-05	1,67E-02	99,83	95,48	3,19E-02
44	Nutter	AIChE	BDH	Gerster	8,10E-03	0,274395	97,05	2,82E-05	1,67E-02	99,83	94,75	4,43E-02

Exp	Abs. tray	Abs. model	Reg. tray	Reg. model	CO_2 lean loading	CO_2 rich loading	n (reg, CO_2) [%]	H_2S lean loading	H_2S rich loading	n (reg, H_2S) [%]	n (abs, CO_2) [%]	H_2S Sweet [ppm]
45	Nutter	Gerster	BDH	Gerster	8,10E-03	0,274011	97,04	2,83E-05	1,67E-02	99,83	94,61	4,90E-02
46	Nutter	Scheffe	Sieve	Chen-Chuang	4,16E-02	0,307548	86,46	1,73E-03	1,82E-02	90,53	94,60	4,97
47	Nutter	AIChE	Sieve	Chen-Chuang	4,14E-02	0,305194	86,43	1,73E-03	1,82E-02	90,51	93,85	5,20
48	Nutter	Gerster	Sieve	Chen-Chuang	4,14E-02	0,304743	86,42	1,73E-03	1,82E-02	90,51	93,68	5,32

E

Elemental sulphur estimation from tank levels

Since faulty gas flow meters are a known and tedious problem, estimating the sulphur formed in the SRU unit is best done using tank levels. When sulphur is formed in the SRU unit, it flows into a buffer vessel, called a pit. This pit is emptied on an irregular basis by an operator, who switches on and off a pump in the field. When the pit is emptied, one can take the sulphur storage tank level before and after the emptying and estimate with geometry how many tonnes have been formed during that period.

First, an emptying is identified in the DCS system, which can be seen in Figure E.1 as the level decreases and starts to rise again. At the same time, it can be seen that the level rises in the sulphur storage tank.

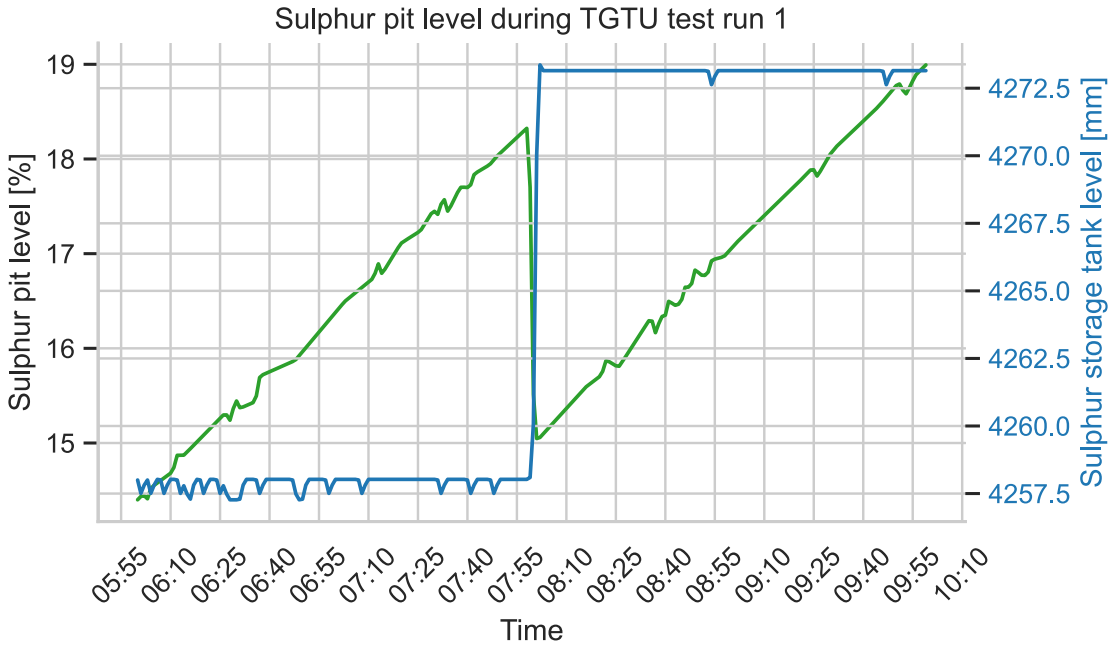

Figure E.1: Process data of pit emptying.

The following nomenclature will be used throughout the appendix:

- ρ_S - Density of elemental sulphur, 1865 kg/m^3

- D_{tank} - Inside diameter of sulphur storage tank
- $L_{T,i}$ - Level of storage tank at t=i in m
- $L_{P,i}$ - Level of sulphur pit at t=i in %

If one assumes that the tank structure is linear, the following Equation E.1 can be applied, which calculates how many tonnes of sulphur the tank was filled with in a particular pit emptying:

$$\text{Tonne elemental sulphur in tank} = (L_{T,1} - L_{T,0}) * \pi * (\frac{D_{tank}}{2})^2 * \rho_S \tag{E.1}$$

The same formula can be put in reverse for the sulphur pit level seen in Equation E.2, it is possible to calculate how many tonnes a per cent unit equals:

$$\text{Tonne sulphur/\% in pit} = \frac{\text{Tonne elemental sulphur in tank}}{L_{T,1} - L_{T,0}} \tag{E.2}$$

With the results from Equation E.2, it is possible to extrapolate this over some time, to approximate how much sulphur is formed in the SRU unit. Approximations differ between different pit emptyings, therefore, a span is appropriate.

DEPARTMENT OF SPACE, EARTH AND ENVIRONMENT
CHALMERS UNIVERSITY OF TECHNOLOGY
Gothenburg, Sweden
www.chalmers.se

CHALMERS
UNIVERSITY OF TECHNOLOGY